

000 001 002 003 004 005 006 007 008 009 010 011 012 013 014 015 016 017 018 019 020 021 022 023 024 025 026 027 028 029 030 031 032 033 034 035 036 037 038 039 040 041 042 043 044 045 046 047 048 049 050 051 052 053 TACKLING FAKE FORGETTING THROUGH UNCERTAINTY QUANTIFICATION

005 **Anonymous authors**

006 Paper under double-blind review

ABSTRACT

012 Machine unlearning seeks to remove the influence of specified data from a trained
013 model. While metrics such as unlearning accuracy (UA) and membership inference
014 attack (MIA) provide baselines for assessing unlearning performance, they fall short
015 of evaluating the reliability of forgetting. In this paper, we find that the data points
016 misclassified by UA and MIA still have their ground truth labels included in the
017 prediction set from the uncertainty quantification perspective, which raises the issue
018 of fake forgetting. To address this issue, we propose two novel metrics inspired by
019 conformal prediction that provide a more reliable evaluation of forgetting quality.
020 Building on these insights, we further propose an unlearning framework that
021 integrates conformal prediction into the Carlini & Wagner adversarial attack loss,
022 which can effectively push the ground truth label out of the conformal prediction
023 set. Through extensive experiments on image classification tasks, we demonstrate
024 both the effectiveness of our proposed metrics and the superiority of our framework.
025 Code is available at <https://anonymous.4open.science/r/MUCP-60E4>.

1 INTRODUCTION

026 Machine unlearning has become essential for data privacy, particularly under regulations such as
027 the GDPR Bourtoule et al. (2021), which grant individuals the right to have their data erased. This
028 creates a strong demand for methods that enable models to behave as if certain data were never
029 used during training. Beyond privacy, unlearning also serves as a tool for mitigating harmful biases
030 and stereotypes in models. Existing post hoc machine unlearning methods can be categorized into
031 training-based Graves et al. (2021); Tarun et al. (2023); Thudi et al. (2022); Warnecke et al. (2021)
032 and training-free Foster et al. (2024); Golatkar et al. (2021; 2020); Guo et al. (2019); Nguyen et al.
033 (2020); Sekhari et al. (2021) approaches, depending on whether they require any model training steps
034 during the unlearning process Foster et al. (2024).

035 To measure the forgetting quality and predictive performance of an unlearning model, several
036 unlearning metrics have been proposed Hayes et al. (2025); Cao & Yang (2015); Chen et al. (2021);
037 Kashev (2021); Shokri et al. (2017). However, existing unlearning metrics, such as unlearning
038 accuracy (UA) and membership inference attack (MIA), fall short in fully evaluating forgetting
039 reliability — these metrics primarily focus on whether models can predict forget data accurately
040 **without sufficiently considering uncertainty and confidence level**. In a nutshell, misclassifying the
041 forget data does not mean that the model has completely forgotten it to some extent.

042 To verify this view, conformal prediction Lei & Wasserman (2014); Papadopoulos et al. (2002) as an
043 uncertainty quantification technique, is applied in our work to recover the misclassified data in UA and
044 MIA. Through extensive experiments, we find that although the model misclassifies part of the forget
045 data from the UA and MIA perspectives, **over 50% of these misclassified data instances still appear**
046 **in the conformal prediction set and can be easily recovered, which exposes a fake forgetting**
047 **issue**. As shown in Figure 1, the important features of prediction visualize this fake forgetting issue
048 by using Grad-CAM Selvaraju et al. (2017). Despite the Finetune method misclassifying the forget
049 data, the Grad-CAM maps still focus heavily on the important features of the object itself since the
050 true label is included in the prediction set. In contrast, when our unlearning method removes the true
051 label from the set, activation regions shift significantly away from the object’s key features. This
052 confirms that forgetting quality improves if the true label can be excluded from the prediction set.

Based on the above insights, we design two novel metrics **CR** and **MIACR** that more effectively capture the uncertainty and robustness of unlearning performance inspired by conformal prediction to tackle the fake forgetting issue. Additionally, motivated by conformal prediction insights about fake forgetting and Carlini & Wagner (C&W) attack loss Carlini & Wagner (2017), we propose a general unlearning framework, which can improve existing training-based unlearning methods and promote reliable forgetting. Grad-CAM maps of our method in Figure 1 reveal that **once the true label no longer falls within the conformal prediction set, the activation regions shift significantly**. To sum up, our contributions are as follows:

- Our analysis reveals that conformal prediction can recover a substantial portion of data previously classified as forgotten by existing unlearning metrics. This fake forgetting issue underscores critical limitations in existing unlearning evaluation methodologies.
- We design two novel metrics to address the limitations motivated by conformal prediction.
- We propose an unlearning framework motivated by conformal prediction and C&W loss, enhancing existing training-based unlearning methods over both existing and our metrics.

2 ENHANCING METRICS FOR MACHINE UNLEARNING BASED ON CONFORMAL PREDICTION

2.1 PRELIMINARIES AND NOTATIONS

Machine Unlearning. In our work, we focus on the image classification task, which is widely used in prior literature Shen et al. (2024); Zhao et al. (2024). Two forgetting scenarios are mainly considered in this work: (i) *random data forgetting* focuses on randomly forgetting specific data instances within the training data, and (ii) *class-wise forgetting* aims to remove all data information associated with an entire class. We also show the results of the subclass-wise forgetting scenario in Table 10 in Appendix. Let \mathcal{D}_{train} denote the original training data used to obtain an original model θ_o . We split the whole training data \mathcal{D}_{train} into two subsets, forget data \mathcal{D}_f and retain data $\mathcal{D}_r = \mathcal{D}_{train} \setminus \mathcal{D}_f$. Let \mathcal{D}_{test} represent test data. θ_u denotes the model after the unlearning process.

Conformal Prediction. Conformal prediction is proposed to quantify uncertainty, providing prediction sets that contain the ground truth label with a theoretically guaranteed probability Angelopoulos & Bates (2021). Among the various types of conformal prediction, this work mainly focuses on split conformal prediction (SCP)¹ since it is the most straightforward and easy-to-implement approach. We also report results of other conformal prediction techniques in Appendix F. To construct a conformal prediction set, SCP involves four steps on the unlearning model:

1. *Calibration Data.* SCP first chooses unseen data as calibration data, which must be held out from both the training and test sets to ensure independence.
2. *Non-conformity Score.* In our work, we follow the conventional choice and set the non-conformity score as

$$S(\mathbf{x}, y_i) = 1 - p_i(\mathbf{x}), \quad (1)$$

where $p_i(\mathbf{x})$ represents the probability of different class y_i .

¹Note that while the goal is to remove the influence of the forget data so that it behaves similarly to the calibration data, the exchangeability property may not always hold in machine unlearning settings. Here, we are directly leveraging the concept of conformal prediction to evaluate machine unlearning performance.

108
 109
 110
 111
 112
 113
 114
 115
 116
 117

3. *Quantile Computation.* Given a target miscoverage rate $\alpha \in [0, 1]$, SCP obtains threshold \hat{q} by taking the $1 - \alpha$ quantile of the non-conformity score of the ground truth labels y_t on the calibration data $(\mathbf{x}, y_t) \in \mathcal{D}_c$,

$$\hat{q} = \text{Quantile}_{1-\alpha}(S(\mathbf{x}, y_t)). \quad (2)$$

4. *Prediction Set.* For the data point \mathbf{x} that needs to be tested, labels with non-conformity scores lower than the threshold \hat{q} are selected for the final prediction set:

$$\mathbb{C}(\mathbf{x}) = \{y_i : S(\mathbf{x}, y_i) \leq \hat{q}\}, \quad (3)$$

2.2 IDENTIFYING FAKE FORGETTING IN EXISTING UNLEARNING METRICS

In this section, we show that a conformal prediction-based recovery technique can reconstruct the true label with high probability even when one forget data point is misclassified. This highlights a critical blind spot in existing UA and MIA metrics from the perspective of uncertainty quantification. The first key question we pose is as follows:

(Q1) Can we recover the data that is identified as forgotten by the metrics UA and MIA?

If the ground truth of forget data falls within the conformal prediction set, we consider the recovery successful. Thus, **fake forgetting is defined as the scenario where a data point identified as forgotten by model prediction can be recovered by conformal prediction.**

To substantiate our claim, we first apply metrics: unlearning accuracy (**UA**, i.e., $1 - \text{the accuracy on forget data}$), retain accuracy (**RA**, i.e., accuracy on retain data), test accuracy (**TA**, i.e., accuracy on test data), and membership inference attack (**MIA**). See Appendix C for MIA implementation details. We evaluate 3 classic unlearning methods, Retrain (**RT**), Finetune (**FT**) Warnecke et al. (2021), and Random Label (**RL**)

Graves et al. (2021). See Appendix A for a detailed introduction to the baselines. The results are trained on CIFAR-10 with ResNet-18 in a random data forgetting scenario. In Table 1, the UA and MIA results suggest that the models fail to correctly classify part of the forget data and identify membership. However, can higher UA and lower MIA fully guarantee that these forget data points do not appear in any form within the model’s predictions?

We employ conformal prediction to investigate whether we can recover forget data’s ground truth, specifically, whether the ground truth labels still appear within the conformal prediction sets. The confidence level and calibration set size are set to 95% and 2000 respectively. In Table 2, we count the number of data points that are identified as truly forgotten by UA and MIA (marked as *mis-label*) and count how many of these *mis-label* points can still be recovered (marked as *in-set*). The **results of UA** reveal that even though the model misclassifies part of the forget data, on average 54.6% of these misclassified data instances are still recovered by conformal prediction. Even for the RT baseline, UA does not reliably assess whether a data point has truly been forgotten, since 30.6% of UA misclassified data points can still be recovered by conformal prediction. This finding demonstrates that a high UA does not mean the model has truly forgotten the data, and thus relying solely on UA to evaluate the forgetting quality is fragile. A similar phenomenon occurs on **results of MIA**. In MIA, ‘0’ indicates a data point is forgotten, while ‘1’ means it is still identified as a training member. The *mis-label* column of MIA refers to the number of data points that are predicted as ‘0’. The *in-set* here refers to the number of *mis-label* data points whose conformal prediction set still includes ‘1’. Thus, the *recover ratio* indicates that, although the MIA fails to identify an average of 18.33% of the forget data as training membership,

Table 1: Unlearning performance measured by existing metrics across RT, FT and RL methods. All values in percent (%). The sign \uparrow (\downarrow) represents the greater (smaller) is better.

Methods	10% Random Forgetting				50% Random Forgetting			
	UA \uparrow	RA \uparrow	TA \uparrow	MIA \downarrow	UA \uparrow	RA \uparrow	TA \uparrow	MIA \downarrow
RT	8.62	99.69	91.83	86.92	10.98	99.80	89.16	82.79
FT	3.84	98.14	91.57	92.00	2.59	99.08	91.77	92.92
RL	7.55	97.41	90.60	74.21	10.48	93.91	85.78	61.15

Table 2: Mis-label (mis-classification) count and in-set ratio of UA and MIA metrics for RT, FT and RL on **CIFAR-10** with **ResNet-18** under **10%** and **50% random data forgetting** scenarios. In all settings, over 30% of mis-label data remains within the conformal prediction set in both UA and MIA. More results of other unlearning methods can be found in Appendix D.

Methods	10% Random Forgetting			50% Random Forgetting		
	Mis-label \uparrow	In-set \downarrow	Ratio \downarrow	Mis-label \uparrow	In-set \downarrow	Ratio \downarrow
Mis-label and In-set Ratio of UA						
RT	431	132	30.6%	2,745	1,573	57.3%
FT	192	112	58.3%	647	431	66.6%
RL	380	173	45.5%	2,625	1,795	68.4%
Mis-label and In-set Ratio of MIA						
RT	654	209	32.0%	4,303	1,391	32.3%
FT	400	216	54.0%	1,769	813	46.0%
RL	1,289	1,011	78.4%	9,713	8,295	85.4%

3

162 conformal prediction can still recover 54.7% of these forget data within prediction sets. For more
 163 results of other unlearning methods, see Table 6 in AppendixD.1.
 164

165 Overall, the high *recover ratio* observed in Tables 2 indicates that misclassified forget data cannot
 166 be considered truly forgotten, as their traces can be readily detected and recovered via conformal
 167 prediction from the perspective of uncertainty quantification. This encloses that **the fake forgetting
 168 issue arises when the true label of misclassified data falls within the conformal prediction set.**

169 2.3 DESIGNING METRICS MOTIVATED BY CONFORMAL PREDICTION

171 Based on the limitation of UA and MIA metrics shown in Section 2.2, it raises a question as follows:
 172

173 **(Q2) Can we develop metrics to address the fake forgetting issue of UA and MIA?**

174 Thus, we propose enhanced UA and MIA metrics that draw intuition from conformal prediction.
 175

176 2.3.1 DEFINITION OF NEW METRICS

178 **Conformal Ratio (CR).** To overcome the fake forgetting inherent in UA, we introduce a novel
 179 metric, CR, which incorporates both coverage and set size in conformal prediction to provide a more
 180 comprehensive evaluation. Before defining CR, we introduce Coverage and Set Size.

181 Given a dataset \mathcal{D} , the definition of **Coverage** is as follows:
 182

$$\text{Coverage} := \frac{1}{|\mathcal{D}|} \sum_{(\mathbf{x}, y_t) \in \mathcal{D}} \mathbb{I}(y_t \in \mathbb{C}_m(\mathbf{x})), \quad (4)$$

185 where y_t is the true label of data point \mathbf{x} . Indicator function $\mathbb{I}(\cdot)$ returns 1 if the enclosed condition is
 186 true and 0 otherwise. Coverage reflects the probability that the true label falls within the prediction
 187 set $\mathbb{C}_m(\mathbf{x})$. For $\mathcal{D} = \mathcal{D}_f$, high coverage indicates that the model retains significant information about
 188 forget data, suggesting fake forgetting.
 189

190 Given a dataset \mathcal{D} , **Set Size** is defined as follows:
 191

$$\text{Set Size} := \frac{1}{|\mathcal{D}|} \sum_{(\mathbf{x}, y_t) \in \mathcal{D}} |\mathbb{C}_m(\mathbf{x})|, \quad (5)$$

194 where $\mathbb{C}_b(\mathbf{x})$ is the conformal prediction set in the multi-class classification task and $|\mathbb{C}_m(\mathbf{x})|$ denotes
 195 the set size of data point \mathbf{x} . When $y_t \in \mathbb{C}_m(\mathbf{x})$, a small set size indicates that fewer non-ground truth
 196 classes are included in the prediction set, reflecting stronger fake forgetting.
 197

198 Based on Coverage and Set Size, we introduce the definition of **CR** for a dataset \mathcal{D} as follows:
 199

$$\text{CR} := \frac{\text{Coverage}}{\text{Set Size}} = \frac{\sum_{(\mathbf{x}, y_t) \in \mathcal{D}} \mathbb{I}(y_t \in \mathbb{C}_m(\mathbf{x}))}{\sum_{(\mathbf{x}, y_t) \in \mathcal{D}} |\mathbb{C}_m(\mathbf{x})|}. \quad (6)$$

201 CR balances the information captured by Coverage and Set Size. A lower CR value implies stronger
 202 forgetting. CR is inspired by conformal prediction, which is proposed to assess the model’s behavior
 203 on new and unseen data, not on the training data. Thus, we emphasize that CR only measures forget
 204 data \mathcal{D}_f and test data \mathcal{D}_{test} .
 205

206 **MIA Conformal Ratio (MIACR).** MIACR is proposed to address the limitation of the existing
 207 MIA metric. Among three potential conformal prediction sets $\{0\}$, $\{1\}$, and $\{0, 1\}$, only set $\{0\}$ is an
 208 ideal case for MIA, because the presence of ‘1’ represents that the data point can still be recognised
 209 as a training member. Therefore, we introduce a new metric **MIACR** as:
 210

$$\text{MIACR} := \frac{1}{|\mathcal{D}_f|} \sum_{(\mathbf{x}, y_t) \in \mathcal{D}_f} \mathbb{I}(\mathbb{C}_b(\mathbf{x}) = \{0\}), \quad (7)$$

213 where $\mathbb{C}_b(\mathbf{x})$ is the conformal prediction set in the binary classification task. $\mathbb{C}_b(\mathbf{x}) = \{0\}$ denotes
 214 prediction set is exactly $\{0\}$. A higher MIACR score indicates a stronger forgetting. Under MIA,
 215 a data point is considered forgotten once the logit for label ‘0’ exceeds that for label ‘1’. However,
 this criterion is often fragile. If the model’s conformal prediction set for a forgetting data point still

216 includes both $\{0, 1\}$, it indicates that the model retains a level of uncertainty and has not completely
 217 purged the data's membership information. To address this, MIACR enforces a stricter rule, requiring
 218 that label '1' be entirely absent from the prediction set, providing a more rigorous assessment of
 219 membership status and forgetting quality.

220 **Superiority of Our Metrics.** Existing accuracy-based metrics UA and MIA suffer from a fake
 221 forgetting issue, since true labels of misclassified data points may still remain within the prediction
 222 set. In contrast, our metrics CR and MIACR address this issue by examining the entire conformal
 223 prediction set, providing a more reliable evaluation of forgetting quality. Besides evidence in Tables 2,
 224 Figures 7–10 in the Appendix also support this superiority of our metrics.

Evaluation Criteria of Our Metrics

227 We consider two different criteria² to measure unlearning performance with our metrics,

228 **① Gap to RT Criterion:** A lower gap to the RT method is better for both CR and MIACR
 229 metrics. The gap relative to RT is represented in blue text (•) in our result tables.

230 **② Limit-Based Criterion:** For the CR, a lower CR value of forget data \mathcal{D}_f indicates stronger
 231 forgetting performance, while a higher CR value of \mathcal{D}_{test} represents higher preserved model
 232 utility. For the MIACR, a higher MIACR value for \mathcal{D}_f reflects better unlearning effectiveness.

2.3.2 DISCUSSION OF CONFIDENCE LEVEL AND CALIBRATION SET SIZE

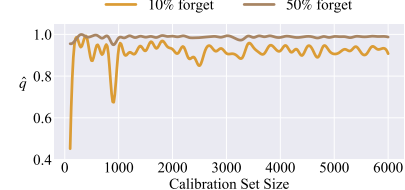
236 In conformal prediction, the confidence level $1 - \alpha$ (i.e.,
 237 miscoverage rate α) and calibration set size are two factors.
 238 We next discuss the suitable settings for the confidence level
 239 and calibration set size, and the rationale behind them.

240 **Confidence Level $1 - \alpha$.** A smaller miscoverage rate α , i.e.,
 241 a higher confidence level $1 - \alpha$, guarantees more reliable cov-
 242 erage. In the conformal prediction related works Angelopou-
 243 los & Bates (2021); Papadopoulos et al. (2002); Romano
 244 et al. (2020a); Tailor et al., $\alpha = 0.05$ is widely adopted
 245 as a standard in most cases, reflecting its common use in
 246 statistical hypothesis testing to balance false positives and
 247 practical usability. Following prior work, we set $\alpha = 0.05$ by default,
 248 while also reporting results for higher values (0.10, 0.15, and 0.20) in Appendices D.3 and D.4 to account for scenarios where a more
 249 relaxed confidence level is needed. Unless otherwise noted, all analyses use the default $\alpha = 0.05$.

250 **Calibration Set Size.** A portion of the validation data is set aside as calibration data, ensuring
 251 it remains independent from both the training and test data. The calibration set must be sufficient
 252 to avoid abnormal \hat{q} values caused by outliers from small samples, which can destabilize coverage
 253 estimates. Figure 2 illustrates the stability of \hat{q} across varying calibration set sizes. The results
 254 are smoothed using a B-spline. We implement them on CIFAR-10 with ResNet-18 in 10% and
 255 50% random data forgetting scenarios. The results show that for different settings using ResNet-18
 256 on CIFAR-10, after the calibration set size is larger than 1000, abnormal \hat{q} values do not occur
 257 anymore, and a stable threshold \hat{q} can be obtained. Similarly, we analyze the calibration set size of
 258 the class-wise forgetting scenario and find that fewer calibration data points are required compared to
 259 random data forgetting. This is because the targeted class forgetting reduces the complexity of the
 260 distribution, unlike the broader variability introduced by random data forgetting.

3 ENHANCING MACHINE UNLEARNING VIA CONFORMAL PREDICTION

263 Based on the findings in Section 2.2, we observe that existing training-based unlearning methods are
 264 typically optimized with respect to loss functions that do not directly support the improvement of
 265 forgetting quality from our fake forgetting perspective. Specifically, the **optimization objectives of**
 266 **existing methods fail to ensure that the ground truth labels are sufficiently pushed out of the**
 267 **conformal prediction set**, which is key to overcoming fake forgetting. This raises a critical question:



268 Figure 2: The stability of \hat{q} in different
 269 calibration set sizes. When the calibration
 270 set size is greater than 2000, the fluctua-
 271 tions of \hat{q} remain within a stable range.

²The appropriate evaluation criteria vary across unlearning application scenarios Kurmanji et al. (2023): criterion ① is particularly relevant for user privacy scenario, while criterion ② focuses on bias removal scenario.

270
 271 **(Q4) Can we explore advanced unlearning techniques via conformal prediction to optimize the**
 272 **existing unlearning model's forgetting quality?**

273 Therefore, we propose a novel and general conformal prediction-based unlearning framework (**CPU**)
 274 tailored for training-based unlearning methods, aimed at enhancing their forgetting quality. A key
 275 insight driving our framework is to overcome the issue exposed by fake forgetting. This emphasizes
 276 that the non-conformity scores of ground truth labels should be pushed beyond the conformal
 277 prediction threshold \hat{q} . Interestingly, this goal aligns naturally with the design of the C&W attack
 278 loss Carlini & Wagner (2017), which motivates our creative adaptation to the unlearning scenario.
 279

280 Let us first apply the original C&W loss directly to the unlearning scenario, without yet incorporating
 281 conformal prediction. For the forget data \mathcal{D}_f , the goal of the unlearning loss is to decrease the model's
 282 confidence in the true labels of \mathcal{D}_f . Based on this, the C&W-inspired unlearning loss is defined as:
 283

$$\mathcal{L}_{\text{cw}}(\mathbf{x}, y_t) = \max\{p_t(\mathbf{x}) - \max_{i \neq t}\{p_i(\mathbf{x})\}, -\Delta\}, \quad (8)$$

284 where $(\mathbf{x}, y_t) \in \mathcal{D}_f$ and $\max\{\cdot\}$ is a maximum operator that selects the largest value from the set.
 285 $p_i(\mathbf{x})$ is the probability of class y_i , and $p_t(\mathbf{x})$ refers specifically to the probability assigned to the true
 286 label y_t . We denote $\max_{i \neq t}\{p_i(\mathbf{x})\}$ as the highest probability value of the non-ground truth classes.
 287 This loss \mathcal{L}_{cw} maximizes the difference between the highest probability value for class y_i ($i \neq t$)
 288 and the probability value for the true class y_t . It tries to decrease the probability of the true class
 289 y_t and further increase that of the class y_i with the highest probability. The margin parameter Δ
 290 controls the enforced margin between the true class and the strongest competing class. When the
 291 $\max_{i \neq t}\{p_i(\mathbf{x})\} - p_t(\mathbf{x}) < \Delta$, this loss encourages the model to decrease the true label's probability
 292 $p_t(\mathbf{x})$. Increasing the value of Δ further increase the margin between $\max_{i \neq t}\{p_i(\mathbf{x})\}$ and $p_t(\mathbf{x})$.
 293

294 With this C&W loss, we can indeed reduce the probability assigned to the true label y_t , thereby
 295 compelling the model to misclassify the data point into another class y_i . However, this loss still
 296 fails to guarantee that the true label y_t can be excluded from the conformal prediction set. If we
 297 let the threshold in conformal prediction play the role of $\max_{i \neq t}\{p_i(\mathbf{x})\}$ in Eq. 8, and push the
 298 non-conformity score of y_t further away from this threshold, the above issue can be effectively
 299 resolved. Therefore, we further improve the C&W-inspired unlearning loss function by combining
 300 conformal prediction.

301 In conformal prediction, calibration data helps in estimating non-conformity scores and determining
 302 a threshold to ensure valid statistical guarantees about the model's uncertainty estimates. A portion
 303 of calibration data \mathcal{D}'_c can be reserved for the unlearning phase, which is kept separate from the
 304 calibration data \mathcal{D}_c used in the evaluation phase. With calibration data \mathcal{D}'_c , the threshold \bar{q} for the
 305 unlearning phase is easily calculated given an α . Given \bar{q} , by revising C&W-inspired unlearning loss
 306 with a calibration step, a general unlearning loss function is defined as follows:
 307

$$\mathcal{L}_{\text{unlearn}}(\mathbf{x}, y_t) = \max\{\bar{q} - S(\mathbf{x}, y_t), -\Delta\}. \quad (9)$$

308 We replace probability $p_t(\mathbf{x})$ and $\max_{i \neq t}\{p_i(\mathbf{x})\}$ in Eq. 8 with the threshold \bar{q} and non-conformity
 309 score $S(\mathbf{x}, y_t)$ respectively. \bar{q} is updated in each training epoch to obtain an accurate value. Since \bar{q} is
 310 computed merely as a quantile, this process incurs negligible computational overhead (experimental
 311 evidence is provided in Appendix E.2).

312 The loss $\mathcal{L}_{\text{unlearn}}$ adheres to the same principle of \mathcal{L}_{cw} , which encourages $S(\mathbf{x}, y_t) - \bar{q} \geq \Delta$. It helps
 313 to increase the non-conformity score $S(\mathbf{x}, y_t)$ of the true label y_t to surpass the threshold \bar{q} . As an
 314 improvement over the loss \mathcal{L}_{cw} , the loss $\mathcal{L}_{\text{unlearn}}$ makes it more difficult for the model to include the
 315 true label in conformal prediction set. In this loss, even a small value of Δ is sufficient to achieve
 316 the desired effect, because the true label y_t is excluded from the conformal prediction set once its
 317 non-conformity score $S(\mathbf{x}, y_t)$ exceeds the threshold \bar{q} . Therefore, in our work, we set $\Delta = 0.01$.
 318

319 As a general framework, to preserve the efficacy of specific unlearning methods themselves, we
 320 reserve their original loss $\mathcal{L}_{\text{original}}$ in our framework. Consequently, we combine these terms to form
 321 the final objective loss function as:
 322

$$\mathcal{L}_{\text{total}} = \mathcal{L}_{\text{original}} + \lambda \cdot \mathcal{L}_{\text{unlearn}}, \quad (10)$$

323 where λ is a hyperparameter that controls the forgetting degree.

324 Table 3: Unlearning performance on **CIFAR-10** with **ResNet-18** and **Tiny ImageNet** with **ViT** in **10% random**
 325 **data forgetting**. The results are average values from 3 independent trials and the standard deviation values
 326 are reported in Appendix D. For evaluation criterion **1**, performance differences compared to the RT method
 327 are highlighted with **(•)**. For clarity in observing criterion **2**, the sign \uparrow represents greater is better, while \downarrow
 328 denotes ideally small. It shows the unlearning methods that excel under the existing metric UA do not necessarily
 329 perform well under our CR metric due to the fake unlearning issue.

Methods	Existing Metrics			Coverage		Set Size		CR	
	UA \uparrow	RA \uparrow	TA \uparrow	$\mathcal{D}_f \downarrow$	$\mathcal{D}_{test} \uparrow$	$\mathcal{D}_f \uparrow$	$\mathcal{D}_{test} \downarrow$	$\mathcal{D}_f \downarrow$	$\mathcal{D}_{test} \uparrow$
CIFAR-10 with ResNet-18									
RT	8.6% (0.0)	99.7% (0.0)	91.8% (0.0)	0.941 (0.000)	0.944 (0.000)	1.089 (0.000)	1.074 (0.000)	0.864 (0.000)	0.879 (0.000)
FT	3.8% (4.8)	98.1% (1.6)	91.6% (0.2)	0.994 (0.053)	0.951 (0.007)	1.008 (0.081)	1.026 (0.048)	0.986 (0.122)	0.927 (0.048)
RL	7.6% (1.0)	97.4% (2.3)	90.6% (1.2)	0.970 (0.029)	0.949 (0.005)	1.242 (0.153)	1.197 (0.123)	0.788 (0.076)	0.796 (0.083)
GA	0.6% (8.0)	99.5% (0.2)	94.1% (2.3)	0.994 (0.053)	0.945 (0.001)	1.002 (0.087)	1.009 (0.065)	0.994 (0.130)	0.936 (0.057)
Teacher	0.8% (7.8)	99.4% (0.3)	93.5% (1.7)	0.991 (0.050)	0.941 (0.003)	1.003 (0.086)	1.021 (0.053)	0.993 (0.129)	0.922 (0.043)
SSD	0.5% (8.1)	99.5% (0.2)	94.2% (2.4)	0.996 (0.055)	0.945 (0.001)	0.999 (0.090)	1.008 (0.066)	0.994 (0.130)	0.936 (0.057)
NegGrad+	8.7% (0.1)	98.8% (0.9)	92.2% (0.4)	0.934 (0.007)	0.948 (0.004)	1.068 (0.021)	1.086 (0.012)	0.875 (0.011)	0.873 (0.006)
Salun	3.7% (4.9)	98.9% (0.8)	91.8% (0.0)	0.987 (0.046)	0.950 (0.006)	1.132 (0.043)	1.143 (0.069)	0.872 (0.008)	0.832 (0.047)
SFRon	4.8% (3.8)	97.4% (2.3)	91.4% (0.4)	0.977 (0.036)	0.953 (0.009)	1.100 (0.011)	1.143 (0.069)	0.889 (0.025)	0.834 (0.045)
Tiny ImageNet with ViT									
RT	14.7% (0.0)	98.8% (0.0)	86.0% (0.0)	0.944 (0.000)	0.949 (0.000)	1.876 (0.000)	1.840 (0.000)	0.503 (0.000)	0.516 (0.000)
FT	6.9% (7.8)	97.9% (0.9)	84.1% (1.9)	0.994 (0.050)	0.950 (0.001)	2.133 (0.257)	2.440 (0.600)	0.466 (0.037)	0.389 (0.127)
RL	26.9% (12.2)	96.0% (2.8)	81.4% (4.6)	0.969 (0.025)	0.952 (0.003)	17.890 (16.014)	8.572 (6.732)	0.054 (0.449)	0.111 (0.405)
GA	3.2% (11.5)	97.4% (1.4)	84.9% (1.1)	0.996 (0.052)	0.947 (0.002)	1.539 (0.337)	2.018 (0.178)	0.647 (0.144)	0.469 (0.047)
Teacher	17.3% (2.6)	86.7% (12.1)	79.0% (7.0)	0.977 (0.033)	0.956 (0.007)	5.473 (3.597)	5.080 (3.240)	0.179 (0.324)	0.188 (0.328)
SSD	1.5% (13.2)	98.5% (0.3)	86.1% (0.1)	0.998 (0.054)	0.950 (0.001)	1.354 (0.522)	1.827 (0.013)	0.737 (0.234)	0.520 (0.004)
NegGrad+	19.4% (4.7)	98.3% (0.5)	84.0% (2.0)	0.999 (0.055)	0.890 (0.059)	0.949 (0.927)	1.614 (0.227)	1.052 (0.823)	0.552 (1.289)
Salun	9.2% (5.5)	97.7% (1.1)	83.6% (2.4)	0.995 (0.051)	0.964 (0.015)	2.803 (0.927)	2.726 (0.886)	0.528 (1.347)	0.376 (1.464)
SFRon	9.3% (5.4)	97.0% (1.8)	83.9% (2.1)	0.989 (0.045)	0.948 (0.001)	2.000 (0.124)	2.208 (0.368)	0.495 (0.008)	0.429 (0.086)

4 EXPERIMENT

4.1 EXPERIMENTAL SETTING

Datasets and Models. We focus on the image classification task and report experiments on CIFAR-10 Krizhevsky (2009) and Tiny ImageNet Le & Yang (2015) datasets with ResNet-18 He et al. (2016) and ViT Dosovitskiy et al. (2021) architectures.

Baselines and Metrics. We employ **9 different unlearning methods**, including **RT**, **FT** Warnecke et al. (2021), **RL** Graves et al. (2021), **Gradient Ascent** (GA) Thudi et al. (2022), **Bad Teacher (Teacher)** Tarun et al. (2023), **SSD** Foster et al. (2024), **NegGrad+** Kurmanji et al. (2023), **Salun** Fan et al. (2024b) and **SFRon** Huang et al. (2025). See Appendix A for a detailed overview of these unlearning methods. We evaluate the performance of various unlearning methods using the existing metrics, including **UA**, **RA**, **TA**, **MIA**, as well as our proposed metrics **CR** and **MIACR**. See Appendix C for the detailed introduction to MIA and our implementation.

Implementation Details. For hyperparameters, we set the miscoverage rate $\alpha \in \{0.05, 0.10, 0.15, 0.20\}$. Results for $\alpha = 0.05$ are reported in the main paper, while results for $\alpha \in \{0.10, 0.15, 0.20\}$ are provided in Appendix D. The margin parameter $\Delta = 0.01$, unlearning loss weight $\lambda \in [0, 0.2, 0.5, 1]$. Additional training and baseline setup details are included in Appendix B.

4.2 MEASURE UNLEARNING METHODS VIA NEW METRICS

In this section, we explore how existing unlearning methods perform with the consideration of the fake forgetting perspective. We evaluate the performance of 9 various unlearning methods using the proposed metrics CR and MIACR, together with Coverage and Set Size. The experimental results are presented in Table 3, which summarizes the unlearning performance under 10% random data forgetting scenario on CIFAR-10 and Tiny ImageNet, respectively. See Tables 10 - 17 in Appendix D for additional experimental results on other forgetting scenarios, including class-wise, subclass-wise and worst-case forgetting.

CR Metric. We take the results on CIFAR-10 as an example for analysis of CR on forget data \mathcal{D}_f based on two evaluation criteria proposed in Section 2.3. According to evaluation criterion **1**, the top 4 methods under the UA metric are *NegGrad+*, *RL*, *SFRon*, and *Salun*, as their unlearning accuracy is closest to the RT method. However, this ranking shifts slightly under the CR metric, where the top 4 become *Salun*, *NegGrad+*, *SFRon*, and *RL*. CR metric identifies that Salun performs better in forgetting quality and can deal with the fake forgetting issue well, while RL faces a fake forgetting

situation and performs poorly on our metric CR. This observation suggests that methods excelling in the traditional UA metric may not perform well under the CR metric. **The underlying rationale behind this is that the CR metric takes into account the possibility that the true labels of some misclassified forget data points may still remain within the prediction set.** This observation aligns with the insights we discussed in Section 2.2 regarding the fake forgetting issue of the UA metric.

Regarding evaluation criterion 2, a similar pattern is observed as with criterion 1. Under the UA metric, the top 4 methods in terms of forgetting quality are *NegGrad+*, *RT*, *RL* and *SFRon*. However, under the CR metric, the top 4 shift to *RL*, *RT*, *Salun* and *NegGrad+*. This indicates that some unlearning methods, such as *NegGrad+*, show weak forgetting quality when viewed from the fake forgetting perspective. This also highlights that the CR captures critical scenarios overlooked by UA, specifically the potential retention of true labels within prediction sets for the forget data points. CR ensures a more robust and reliable evaluation for unlearning quality.

MIACR Metric. In Table 4, we show the MIACR results on CIFAR-10 under both 10% and 50% random data forgetting. Under our evaluation criterion 1, most methods show superior MIA and MIACR performance in the 10% forgetting scenario compared to 50% forgetting, because larger forget sets pose greater challenges for unlearning methods. This demonstrates that the general trend of membership leakage risk remains broadly consistent across MIA and MIACR. Under evaluation criterion 2, Salun, which appears optimal under MIA, does not achieve the best performance when assessed by MIACR. In the 10% random forgetting scenario, MIA deems 2,121 data points as truly forgotten by Salun and 423 by SFRon. However, MIACR reveals that 1,848 of the 2,121 points under Salun can still be recovered via conformal prediction, whereas only 121 of the 423 points remain within the prediction set for SFRon.

Overall, the results show that, compared to MIACR, the existing MIA metric still leaves privacy concerns. Although MIA may fail to predict some forget data points as training members, these points can still appear in the conformal prediction set with high confidence. In contrast, **MIACR more strictly controls potential membership leakage risk by measuring the probability that only non-member predictions (i.e., label ‘0’) appear in the prediction set.**

4.3 PERFORMANCE OF OUR UNLEARNING FRAMEWORK

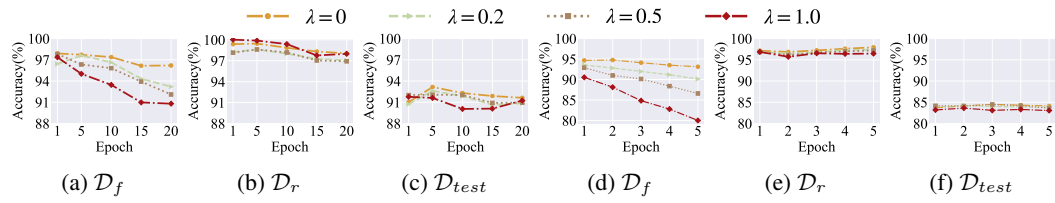
In this experiment, we apply RT, FT, and RL methods to our framework CPU, i.e., CPU-RT, CPU-FT, CPU-RL. Table 5 presents the results for CIFAR-10 with ResNet-18 and Tiny ImageNet with ViT in 10% random data forgetting. We vary λ in the range $[0, 0.2, 0.5, 1]$, where $\lambda = 0$ represents the baseline without our framework applied. See Table 18 in Appendix E for the results of $\lambda = 1$.

From the perspective of evaluation criterion 1, we take CPU-FT as an example for analysis. The gap (blue text (•)) between CPU-FT and RT on the existing metric UA decreases effectively as λ increases. Specifically, the UA gap decreases from 4.8% to 0.7% on CIFAR-10 and from 7.8% to 0.9% on Tiny ImageNet. It is worth noting that the model utility remains relatively stable on the RA and TA results. Similarly, $CR_{\mathcal{D}_f}$ metric is also decreased when $\lambda > 0$. For the average gap across UA, RA, and TA metrics, the CPU-FT method achieves a promising average gap of 1.47 on ResNet-18 when $\lambda = 0.5$, compared to an average gap of 2.2 when $\lambda = 0$. Similarly, on the ViT model, CPU-FT reduces the average gap from 3.53 to 1.63 when $\lambda = 0.5$. It is obvious that our framework can strongly improve forgetting strength. That means the methods that are prone to over-forgetting, such as RL, perform adequately without requiring CPU for additional enhancements under our evaluation criterion 1.

For evaluation criterion 2, when $\lambda = 0.5$, the UA improves by an average of 3.93% on ResNet-18 and 9.23% on ViT over all methods, while TA decreases only slightly by 1.0% and 0.57% on ResNet-18 and ViT respectively. As similarly shown in the CR metric, the value of $CR_{\mathcal{D}_{test}}$ remains nearly unchanged compared to the baseline ($\lambda = 0$) with only 0.03 drop on average, while $CR_{\mathcal{D}_f}$ shows a greater reduction with an average of 0.08 across all methods.

432 Table 5: Performance of our unlearning framework CPU. We show the performance on **CIFAR-10** with
 433 **ResNet-18** and **Tiny ImageNet** with **ViT** in **10% random data forgetting**. $\lambda = 0$ represents the baseline
 434 without our framework applied. It shows our framework significantly improves the forgetting quality, not only
 435 across our metric but also existing metric UA, while preserving stable predictive performance.

Methods	$\lambda = 0$				$\lambda = 0.2$				$\lambda = 0.5$						
	UA \uparrow	RA \uparrow	TA \uparrow	$\text{CR}_{\mathcal{D}_f} \downarrow$	UA \uparrow	RA \uparrow	TA \uparrow	$\text{CR}_{\mathcal{D}_f} \downarrow$	UA \uparrow	RA \uparrow	TA \uparrow	$\text{CR}_{\mathcal{D}_f} \downarrow$			
CIFAR-10 with ResNet-18															
CPU-RT	8.6% ^(0.0)	99.7% ^(0.0)	91.8% ^(0.0)	0.864 ^(0.000)	0.879 ^(0.000)	10.8% ^(2.2)	98.3% ^(1.4)	91.0% ^(0.8)	0.788 ^(0.076)	0.824 ^(0.055)	14.0% ^(5.4)	97.8% ^(1.9)	90.4% ^(0.4)	0.763 ^(0.101)	0.825 ^(0.054)
CPU-FT	3.8% ^(4.8)	98.1% ^(1.6)	91.6% ^(0.2)	0.986 ^(0.122)	0.927 ^(0.048)	6.8% ^(1.8)	97.0% ^(2.7)	90.8% ^(1.0)	0.844 ^(0.020)	0.829 ^(0.050)	7.9% ^(0.7)	96.9% ^(2.8)	90.9% ^(0.9)	0.853 ^(0.011)	0.843 ^(0.036)
CPU-RL	7.6% ^(1.0)	97.4% ^(2.3)	90.6% ^(1.2)	0.788 ^(0.076)	0.796 ^(0.083)	9.7% ^(1.1)	96.6% ^(3.1)	89.4% ^(2.4)	0.709 ^(0.155)	0.736 ^(0.143)	9.9% ^(1.3)	96.9% ^(2.8)	89.7% ^(2.1)	0.708 ^(0.156)	0.731 ^(0.148)
Tiny ImageNet with ViT															
CPU-RT	14.7% ^(0.0)	98.8% ^(0.0)	86.0% ^(0.0)	0.503 ^(0.000)	0.516 ^(0.000)	19.3% ^(4.6)	98.8% ^(0.0)	86.0% ^(0.0)	0.458 ^(0.045)	0.516 ^(0.000)	26.4% ^(11.7)	98.7% ^(0.1)	85.8% ^(0.2)	0.396 ^(0.107)	0.489 ^(0.027)
CPU-FT	6.9% ^(7.8)	97.9% ^(0.9)	84.1% ^(1.9)	0.466 ^(0.037)	0.389 ^(0.127)	9.8% ^(4.9)	97.4% ^(1.4)	83.6% ^(2.4)	0.441 ^(0.062)	0.399 ^(0.117)	13.6% ^(0.9)	97.2% ^(1.6)	83.6% ^(2.4)	0.413 ^(0.090)	0.401 ^(0.115)
CPU-RL	26.9% ^(12.2)	96.0% ^(2.8)	81.4% ^(4.6)	0.054 ^(0.449)	0.111 ^(0.405)	31.8% ^(17.1)	95.3% ^(17.9)	80.9% ^(5.1)	0.051 ^(0.452)	0.111 ^(0.405)	36.2% ^(21.5)	95.3% ^(3.5)	80.4% ^(5.6)	0.051 ^(0.452)	0.121 ^(0.395)



442
 443 Figure 3: CPU-FT accuracy of \mathcal{D}_f , \mathcal{D}_r and \mathcal{D}_{test} under different λ values across each epoch on CIFAR-10
 444 (a-c) and Tiny ImageNet (d-f). As λ increases, accuracy on \mathcal{D}_f drops significantly, while retain and test accuracy
 445 remain stable.

446 Moreover, in Figure 3, we further present the CPU-FT accuracy on forget data \mathcal{D}_f , retain data \mathcal{D}_r and
 447 test data \mathcal{D}_{test} under different λ values across each epoch on Tiny ImageNet with ViT for 10% random
 448 data forgetting. As λ increases, the accuracy on \mathcal{D}_f drops quickly, showing stronger unlearning
 449 effectiveness, while the accuracy on \mathcal{D}_r and \mathcal{D}_{test} remains stable. In summary, the experimental
 450 results demonstrate that our framework notably enhances the forgetting quality while maintaining
 451 stable predictive performance.

452 The experimental results demonstrate a significant improvement in both UA and $\text{CR}_{\mathcal{D}_f}$ across all
 453 methods, reflecting improved forgetting quality as λ increases. Notably, the RA, TA, and $\text{CR}_{\mathcal{D}_{test}}$
 454 values remain relatively stable, indicating that the substantial improvement in forgetting quality does
 455 not compromise the model’s performance.

5 RELATED WORK

464 Machine unlearning has emerged as a vital research topic due to several privacy, regulatory, and
 465 ethical concerns associated with machine learning models. It refers to the process of selectively
 466 removing specific data points from a trained machine learning model. Generally, post-hoc machine
 467 unlearning can be divided into training-based Graves et al. (2021); Tarun et al. (2023); Thudi et al.
 468 (2022); Warnecke et al. (2021) and training-free approaches Foster et al. (2024); Golatkar et al. (2021;
 469 2020); Guo et al. (2019); Nguyen et al. (2020); Sekhari et al. (2021).

470 To evaluate these methods, several unlearning metrics have been proposed, including UA Brophy
 471 & Lowd (2021); Foster et al. (2024) and MIA Chen et al. (2021); Hayes et al. (2025); Shokri et al.
 472 (2017). However, these metrics often fail to account for the confidence of the forgetting quality. To
 473 address this limitation, we improve it in our work motivated by conformal prediction Angelopoulos &
 474 Bates (2021), which stands out among uncertainty quantification techniques for its ability to provide
 475 well-calibrated, reliable confidence measures. As a generic methodology, conformal prediction can
 476 transform the outputs of any black box prediction algorithm into a prediction set. Due to its versatility,
 477 many works have specifically designed numerous conformal prediction methods tailored to particular
 478 prediction problems Lei et al. (2018); Lei & Wasserman (2014); Papadopoulos et al. (2002); Romano
 479 et al. (2020a).

480 One work Becker & Liebig (2022) has primarily focused on parameter-level uncertainty without fully
 481 addressing the broader implications of unlearning on prediction confidence. It assesses the sensitivity
 482 of model parameters to the target data through the Fisher Information Matrix, but they often rely on
 483 computationally intensive operations and may struggle to scale to large models or datasets.

486 **6 CONCLUSION**

488 Motivated by conformal prediction, we introduce new metrics, CR and MIACR, to enhance the
 489 evaluation and reliability of machine unlearning. In addition, our unlearning framework, which
 490 incorporates the adapted C&W loss with conformal prediction, improves unlearning effectiveness.
 491 Together, we provide a more rigorous foundation for privacy-preserving machine learning.

493 **REPRODUCIBILITY STATEMENT**

495 The implementation details are introduced in Appendix A-B and the codes are available at
 496 <https://anonymous.4open.science/r/MUCP-60E4>.
 497

498 **REFERENCES**

500 Anastasios Angelopoulos, Stephen Bates, Jitendra Malik, and Michael I Jordan. Uncertainty sets for
 501 image classifiers using conformal prediction. [arXiv preprint arXiv:2009.14193](https://arxiv.org/abs/2009.14193), 2020.

503 Anastasios N Angelopoulos and Stephen Bates. A gentle introduction to conformal prediction and
 504 distribution-free uncertainty quantification. [arXiv preprint arXiv:2107.07511](https://arxiv.org/abs/2107.07511), 2021.

506 Alexander Becker and Thomas Liebig. Evaluating machine unlearning via epistemic uncertainty.
 507 [arXiv preprint arXiv:2208.10836](https://arxiv.org/abs/2208.10836), 2022.

509 Lucas Bourtoule, Varun Chandrasekaran, Christopher A Choquette-Choo, Hengrui Jia, Adelin Travers,
 510 Baiwu Zhang, David Lie, and Nicolas Papernot. Machine unlearning. In [2021 IEEE Symposium
 511 on Security and Privacy \(SP\)](https://ieeexplore.ieee.org/abstract/document/9537500), pp. 141–159. IEEE, 2021.

512 Jonathan Brophy and Daniel Lowd. Machine unlearning for random forests. In [International
 513 Conference on Machine Learning](https://proceedings.mlr.press/v160/brophy22a.html), pp. 1092–1104. PMLR, 2021.

515 Margarida M Campos, João Calém, Sophia Sklaviadis, Mário AT Figueiredo, and André FT Martins.
 516 Sparse activations as conformal predictors. [arXiv preprint arXiv:2502.14773](https://arxiv.org/abs/2502.14773), 2025.

517 Yinzheng Cao and Junfeng Yang. Towards making systems forget with machine unlearning. In [2015
 518 IEEE symposium on security and privacy](https://ieeexplore.ieee.org/abstract/document/7290510), pp. 463–480. IEEE, 2015.

520 Nicholas Carlini and David Wagner. Towards evaluating the robustness of neural networks. In [2017
 521 ieee symposium on security and privacy \(sp\)](https://ieeexplore.ieee.org/abstract/document/7979059), pp. 39–57. Ieee, 2017.

523 Min Chen, Zhikun Zhang, Tianhao Wang, Michael Backes, Mathias Humbert, and Yang Zhang. When
 524 machine unlearning jeopardizes privacy. In [Proceedings of the 2021 ACM SIGSAC conference
 525 on computer and communications security](https://dl.acm.org/doi/10.1145/3493119.3493130), pp. 896–911, 2021.

526 Alexey Dosovitskiy, Lucas Beyer, Alexander Kolesnikov, Dirk Weissenborn, Xiaohua Zhai, Thomas
 527 Unterthiner, Mostafa Dehghani, Matthias Minderer, Georg Heigold, Sylvain Gelly, Jakob Uszkoreit,
 528 and Neil Houlsby. An image is worth 16x16 words: Transformers for image recognition at scale,
 529 2021. URL <https://arxiv.org/abs/2010.11929>.

531 Chongyu Fan, Jiancheng Liu, Alfred Hero, and Sijia Liu. Challenging forgets: Unveiling the worst-
 532 case forget sets in machine unlearning. In [European Conference on Computer Vision](https://openaccess.thecvf.com/content/ECCV2024/html/Fan_Fan_etal_ECCV24.pdf), pp. 278–297.
 533 Springer, 2024a.

534 Chongyu Fan, Jiancheng Liu, Yihua Zhang, Dennis Wei, Eric Wong, and Sijia Liu. Salun: Em-
 535 powering machine unlearning via gradient-based weight saliency in both image classification and
 536 generation. In [International Conference on Learning Representations](https://openaccess.thecvf.com/content/ICLR2024/html/Fan_Fan_etal_ICLR24.pdf), 2024b.

538 Jack Foster, Stefan Schoepf, and Alexandra Brintrup. Fast machine unlearning without retraining
 539 through selective synaptic dampening. In [Proceedings of the AAAI Conference on Artificial
 Intelligence](https://ojs.aaai.org/index.php/AAAI/article/2043), volume 38, pp. 12043–12051, 2024.

540 Aditya Golatkar, Alessandro Achille, and Stefano Soatto. Forgetting outside the box: Scrubbing deep
 541 networks of information accessible from input-output observations. In European Conference on
 542 Computer Vision, pp. 383–398, 2020.

543 Aditya Golatkar, Alessandro Achille, Avinash Ravichandran, Marzia Polito, and Stefano Soatto.
 544 Mixed-privacy forgetting in deep networks. In Proceedings of the IEEE/CVF conference on
 545 computer vision and pattern recognition, pp. 792–801, 2021.

546 Laura Graves, Vineel Nagisetty, and Vijay Ganesh. Amnesiac machine learning. In Proceedings of
 547 the AAAI Conference on Artificial Intelligence, volume 35, pp. 11516–11524, 2021.

548 Chuan Guo, Tom Goldstein, Awni Hannun, and Laurens Van Der Maaten. Certified data removal
 549 from machine learning models. arXiv preprint arXiv:1911.03030, 2019.

550 Jamie Hayes, Ilia Shumailov, Eleni Triantafillou, Amr Khalifa, and Nicolas Papernot. Inexact
 551 unlearning needs more careful evaluations to avoid a false sense of privacy. In 2025 IEEE
 552 Conference on Secure and Trustworthy Machine Learning (SaTML), pp. 497–519. IEEE, 2025.

553 Kaiming He, Xiangyu Zhang, Shaoqing Ren, and Jian Sun. Identity mappings in deep residual
 554 networks. In Bastian Leibe, Jiri Matas, Nicu Sebe, and Max Welling (eds.), Computer Vision
 555 – ECCV 2016, pp. 630–645, Cham, 2016. Springer International Publishing. ISBN 978-3-319-
 556 46493-0.

557 Jianguo Huang, Huajun Xi, Linjun Zhang, Huaxiu Yao, Yue Qiu, and Hongxin Wei. Conformal
 558 prediction for deep classifier via label ranking. arXiv preprint arXiv:2310.06430, 2023.

559 Zhehao Huang, Xinwen Cheng, JingHao Zheng, Haoran Wang, Zhengbao He, Tao Li, and Xiaolin
 560 Huang. Unified gradient-based machine unlearning with remain geometry enhancement. Advances
 561 in Neural Information Processing Systems, 37:26377–26414, 2025.

562 Jinghan Jia, Jiancheng Liu, Parikshit Ram, Yuguang Yao, Gaowen Liu, Yang Liu, Pranay Sharma,
 563 and Sijia Liu. Model sparsity can simplify machine unlearning. Advances in Neural Information
 564 Processing Systems, 36:51584–51605, 2023.

565 Rasha Kashef. A boosted svm classifier trained by incremental learning and decremental unlearning
 566 approach. Expert Systems with Applications, 167:114154, 2021.

567 Alex Krizhevsky. Learning multiple layers of features from tiny images. 2009. URL <https://api.semanticscholar.org/CorpusID:18268744>.

568 Meghdad Kurmanji, Peter Triantafillou, Jamie Hayes, and Eleni Triantafillou. Towards unbounded
 569 machine unlearning. Advances in neural information processing systems, 36:1957–1987, 2023.

570 Ya Le and Xuan Yang. Tiny imagenet visual recognition challenge. CS 231N, 7(7):3, 2015.

571 Jing Lei and Larry Wasserman. Distribution-free prediction bands for non-parametric regression.
 572 Journal of the Royal Statistical Society Series B: Statistical Methodology, 76(1):71–96, 2014.

573 Jing Lei, Max G’Sell, Alessandro Rinaldo, Ryan J Tibshirani, and Larry Wasserman. Distribution-
 574 free predictive inference for regression. Journal of the American Statistical Association, 113(523):
 575 1094–1111, 2018.

576 Quoc Phong Nguyen, Bryan Kian Hsiang Low, and Patrick Jaillet. Variational bayesian unlearning.
 577 Advances in Neural Information Processing Systems, 33:16025–16036, 2020.

578 Harris Papadopoulos, Kostas Proedrou, Volodya Vovk, and Alex Gammerman. Inductive confi-
 579 dence machines for regression. In Machine learning: ECML 2002: 13th European conference on
 580 machine learning Helsinki, Finland, August 19–23, 2002 proceedings 13, pp. 345–356. Springer,
 581 2002.

582 Yaniv Romano, Matteo Sesia, and Emmanuel Candes. Classification with valid and adaptive coverage.
 583 Advances in Neural Information Processing Systems, 33:3581–3591, 2020a.

584 Yaniv Romano, Matteo Sesia, and Emmanuel Candes. Classification with valid and adaptive coverage.
 585 Advances in neural information processing systems, 33:3581–3591, 2020b.

594 Mauricio Sadinle, Jing Lei, and Larry Wasserman. Least ambiguous set-valued classifiers with
 595 bounded error levels. *Journal of the American Statistical Association*, 114(525):223–234, 2019.
 596

597 Ayush Sekhari, Jayadev Acharya, Gautam Kamath, and Ananda Theertha Suresh. Remember
 598 what you want to forget: Algorithms for machine unlearning. *Advances in Neural Information
 599 Processing Systems*, 34:18075–18086, 2021.

600 Ramprasaath R Selvaraju, Michael Cogswell, Abhishek Das, Ramakrishna Vedantam, Devi Parikh,
 601 and Dhruv Batra. Grad-cam: Visual explanations from deep networks via gradient-based local-
 602 ization. In *Proceedings of the IEEE international conference on computer vision*, pp. 618–626,
 603 2017.

604 Shaofei Shen, Chenhao Zhang, Yawen Zhao, Weitong Chen, Alina Bialkowski, and Miao Xu. Label-
 605 agnostic forgetting: a supervision-free unlearning in deep models. In *12th International Conference
 606 on Learning Representations, ICLR 2024*. International Conference on Learning Representations,
 607 ICLR, 2024.

608

609 Reza Shokri, Marco Stronati, Congzheng Song, and Vitaly Shmatikov. Membership inference attacks
 610 against machine learning models. In *2017 IEEE symposium on security and privacy (SP)*, pp.
 611 3–18. IEEE, 2017.

612 Liwei Song, Reza Shokri, and Prateek Mittal. Privacy risks of securing machine learning models
 613 against adversarial examples. In *Proceedings of the 2019 ACM SIGSAC conference on computer
 614 and communications security*, pp. 241–257, 2019.

615

616 Dharmesh Tailor, Alvaro Correia, Eric Nalisnick, and Christos Louizos. Approximating full con-
 617 formal prediction for neural network regression with gauss-newton influence. In *The Thirteenth
 618 International Conference on Learning Representations*.

619

620 Ayush Kumar Tarun, Vikram Singh Chundawat, Murari Mandal, and Mohan Kankanhalli. Deep
 621 regression unlearning. In *International Conference on Machine Learning*, pp. 33921–33939.
 622 PMLR, 2023.

623

624 Anvith Thudi, Gabriel Deza, Varun Chandrasekaran, and Nicolas Papernot. Unrolling sgd: Un-
 625 derstanding factors influencing machine unlearning. In *2022 IEEE 7th European Symposium on
 626 Security and Privacy (EuroS&P)*, pp. 303–319. IEEE, 2022.

627

628 Alexander Warnecke, Lukas Pirch, Christian Wressnegger, and Konrad Rieck. Machine unlearning
 629 of features and labels. *arXiv preprint arXiv:2108.11577*, 2021.

630

631 Samuel Yeom, Irene Giacomelli, Matt Fredrikson, and Somesh Jha. Privacy risk in machine learn-
 632 ing: Analyzing the connection to overfitting. In *2018 IEEE 31st computer security foundations
 633 symposium (CSF)*, pp. 268–282. IEEE, 2018.

634

635 Kairan Zhao, Meghdad Kurmanji, George-Octavian Bărbulescu, Eleni Triantafillou, and Peter Tri-
 636 antafillou. What makes unlearning hard and what to do about it. *Advances in Neural Information
 637 Processing Systems*, 37:12293–12333, 2024.

638

639

640

641

642

643

644

645

646

647

648 APPENDIX
649650 A BASELINE DETAILS
651

652 We introduce the details of our unlearning baselines as follows : **RT** retrains the model from scratch
 653 using only the remaining dataset \mathcal{D}_r . **FT** Warnecke et al. (2021) fine-tunes the pre-trained model θ_o
 654 on the remaining dataset \mathcal{D}_r . **RL** Graves et al. (2021) fine-tunes the model on the forgetting dataset
 655 \mathcal{D}_f using randomly assigned labels to enforce forgetting. **GA** Thudi et al. (2022) performs gradient
 656 ascent on the forgetting data \mathcal{D}_f , which often harms the model’s utility. **Teacher** Tarun et al. (2023)
 657 distills knowledge from a corrupted teacher model to the student, aiming to uniformly increase the
 658 loss on forgetting samples but often causing catastrophic forgetting. **SSD** Foster et al. (2024) induces
 659 forgetting by identifying and dampening parameters highly associated with the forgetting set using
 660 the Fisher information matrix, without retraining. **NegGrad+** Kurmanji et al. (2023) addresses GA’s
 661 issue by combining fine-tuning on \mathcal{D}_r and gradient ascent on \mathcal{D}_f . **Salun** Fan et al. (2024b) performs
 662 unlearning by optimizing only the salient parameters of the model identified from the random labeled
 663 forgetting data. **SFRon** Huang et al. (2025) embeds the unlearning update into the parameter manifold
 664 shaped by the retained data using Hessian modulation, approximated via a fast-slow update strategy.
 665

666 B SETTING DETAILS
667

668 For CIFAR-10 with ResNet-18 architecture, we train the original model from scratch for 200 epochs
 669 using SGD with a Cosine Annealing learning rate schedule, starting from an initial learning rate
 670 of 0.1. We set the momentum to 0.9 and a batch size of 64. The RT model adopts the same
 671 training configuration. Other models are trained for the following durations: FT for 20 epochs, RL
 672 for 10 epochs, Salun for 10 epochs, GA for 1 epoch (to avoid over-forgetting and significant RA
 673 degradation), NegGrad+ for 10 epochs (reduced to 2 epochs in class-wise scenarios), and SFRon for
 674 10 epochs. All other hyperparameters match those of the original model.

675 For the ViT architecture, we initialize the original model by training a pretrained ViT model for 15
 676 epochs on Tiny ImageNet. We start with a learning rate of 0.001, while other training parameters
 677 match those used for ResNet-18. We use SGD and set the momentum to 0.9 and a batch size of 64.
 678 The RT model follows the same training procedure as the original model. Other models are trained
 679 for the following durations: FT for 5 epochs, RL for 5 epochs, Salun for 5 epochs, GA for 1 epoch,
 680 NegGrad+ for 5 epochs, and SFRon for 5 epochs. All other hyperparameters are consistent with the
 681 original model’s training.

682 For CIFAR-10/Tiny ImageNet, we randomly select 200/50 data points per class (2000/10000 data
 683 points in total) as calibration data \mathcal{D}_c and \mathcal{D}'_c , respectively. The calibration data \mathcal{D}_c does not participate
 684 in the model training or unlearning processes and is only used for calibrating the threshold \hat{q} , while
 685 \mathcal{D}'_c is used in the process of our unlearning framework to generate \bar{q} . All experiments are conducted
 686 on 1 Tesla V100-SXM2 GPU card with 32GB memory in a single node.

687 C MIA IMPLEMENTATION DETAILS
688

689 Following prior works Jia et al. (2023); Kurmanji et al. (2023); Zhao et al. (2024); Song et al. (2019);
 690 Yeom et al. (2018), we adopt a confidence-based membership inference attack to evaluate the privacy
 691 preservation of the unlearning model. Specifically, we construct an MIA predictor by training it on a
 692 balanced dataset sampled from the retain set \mathcal{D}_r (labeled as members) and the test set \mathcal{D}_{test} (labeled
 693 as non-members). The trained support vector classifier (SVC) is then applied to the unlearning model
 694 θ_u during evaluation.

695 To measure unlearning effectiveness, we compute the MIA success rate, which quantifies how many
 696 samples in the forget set \mathcal{D}_f are still predicted as training members by the MIA predictor. Formally,

$$698 \text{MIA} = \frac{\text{TP}}{|\mathcal{D}_f|}, \quad (11)$$

699 700 where TP represents the count of forget samples still identified as training samples and $|\mathcal{D}_f|$ is the
 701 size of the forget data \mathcal{D}_f .

702 Intuitively, since the MIA score reflects the success rate of membership inference attacks on the forget
 703 data, a lower score indicates that less membership information about \mathcal{D}_f is retained in θ_u , implying
 704 stronger privacy preservation and more effective unlearning.
 705

706 D EVALUATING MU METHODS

707 D.1 MIS-LABEL NUMBER AND IN-SET RATIOS

710 Table 6: Mis-label number and in-set ratios of UA and MIA metrics.
 711

712 Methods	713 10% Forgetting			714 50% Forgetting		
	715 Mis-label ↑	716 In-set ↓	717 Ratio ↓	718 Mis-label ↑	719 In-set ↓	720 Ratio ↓
721 Mis-label and In-set Ratio of UA						
722 RT	723 431	724 132	725 30.6%	726 2,745	727 1,573	728 57.3%
729 FT	730 192	731 112	732 58.3%	733 647	734 431	735 66.6%
736 RL	737 380	738 173	739 45.5%	740 2,625	741 1,795	742 68.4%
743 GA	744 30	745 2	746 6.7%	747 150	748 9	749 6.0%
750 Teacher	751 40	752 4	753 10%	754 400	755 37	756 9.3%
757 SSD	758 25	759 2	760 8.0%	761 116	762 9	763 7.8%
764 NegGrad+	765 435	766 115	767 26.4%	768 711	769 249	770 35.5%
772 Salun	773 185	774 117	775 63.2%	776 1,065	777 695	778 65.3%
780 SFRon	781 240	782 125	783 52.1%	784 1,000	785 610	786 61.0%
787 Mis-label and In-set Ratio of MIA						
788 RT	789 654	790 209	791 32.0%	792 4,303	793 1,391	794 32.3%
795 FT	796 400	797 216	798 54.0%	799 1,769	800 813	801 46.0%
802 RL	803 1,289	804 1,011	805 78.4%	806 9,713	807 8,295	808 85.4%
809 GA	810 60	811 10	812 16.7%	813 284	814 31	815 10.9%
816 Teacher	817 638	818 586	819 91.8%	820 1,689	821 895	822 53.0%
824 SSD	825 61	826 11	827 18.0%	828 282	829 24	830 8.5%
832 NegGrad+	833 486	834 106	835 21.8%	836 1,545	837 415	838 26.9%
840 Salun	841 2,121	842 1,848	843 87.1%	844 10,221	845 9,121	846 89.2%
848 SFRon	849 423	850 121	851 28.6%	852 1,871	853 433	854 23.1%

729 Conformal prediction is applied to UA and MIA predictions to determine the number of misclassified
 730 data points (mis-label) and the number of these points that fall within the conformal prediction set
 731 (in-set). We evaluate both the UA and MIA metrics by counting the misclassified data points and
 732 calculating how many of them are included in the conformal prediction set. The detailed results are
 733 presented in Table 6, which is the extended results of Table 2.

735 D.2 DISTRIBUTION COMPARISON OF FORGOTTEN DATA ON UA AND CR

737 As shown in Figures 7-10, we further analyze the probability and loss distributions of ground truth
 738 labels for data identified as truly forgotten by CR (i.e., out-set) and UA (i.e., mis-label), respectively.
 739 The distribution curves are fitted using KDE for clearer visualization. The softmax outputs for
 740 ‘out-set’ are consistently near 0 compared to ‘mis-label’, which strongly suggests that ‘out-set’ more
 741 rigorously captures real forgotten data. In the cross-entropy loss distribution, forgotten data identified
 742 by CR consistently show higher cross-entropy loss than UA. Higher loss indicates better forgetting
 743 quality, which further validates that CR better removes fake forgetting data.

744 D.3 CR METRIC

746 Tables 11 and 12 show the unlearning performance on CIFAR-10 with ResNet-18 in 10% and 50%
 747 random data forgetting scenarios, while Table 13 is the results in class-wise forgetting scenario.
 748 Tables 14 and 15 present the unlearning performance on Tiny ImageNet with ResNet-18 in the
 749 random data forgetting scenario, while Table 16 details the unlearning performance in the class-wise
 750 forgetting scenario. For class-wise forgetting scenario, we note $\mathcal{D}_{test} = \mathcal{D}_{tf} \cup \mathcal{D}_{tr}$. \mathcal{D}_{tf} corresponds
 751 to the test-forget data exclusively containing the forget class, while \mathcal{D}_{tr} represents the test-retain data
 752 within the test data \mathcal{D}_{test} .

753 For all unlearning methods, as α level increases, it results in reduced Coverage and smaller Set Size.
 754 This happens because a higher α loosens the conformal threshold \hat{q} , allowing fewer predictions to be
 755 included within the prediction set for each data point. On the contrary, the CR tends to increase with
 increasing α . Although both Coverage and Set Size may decrease, Set Size often decreases more

significantly. Consequently, the CR value of \mathcal{D}_f generally becomes larger as α increases. It is natural that the adjustment of α affects both Coverage and Set Size. However, the final CR value really depends on the model’s performance itself. For a strict evaluation, we encourage setting α to 0.5.

When α is set to 0.2, most methods show a value of Set Size less than 1 in both Table 11, 12, 14, 15. The intuition behind it is that conformal prediction, as a static predictor, is intrinsically tied to the model’s base prediction performance and accuracy. When the model’s accuracy is significantly higher than the confidence level, conformal prediction can achieve the required coverage with ease. In fact, it can generate partial empty prediction sets for some data points while still meeting the target coverage. Thus, the choice of α is crucial. Overly high α values may skew evaluation results by failing to let CR accurately reflect model performance. Therefore, we emphasize that a small α is generally appropriate for most unlearning scenarios.

Notably, the insights gained from the random data forgetting scenario can also be extended to the class-wise forgetting scenario. Additionally, in the class-wise scenario, some unlearning methods like RT and RL with UA = 100% and CR approaching 0% indicate they are truly effective at forgetting the specified class.

D.4 MIACR METRIC

Table 17 presents the performance of 9 machine unlearning methods on CIFAR-10 in ResNet-18, evaluated with the MIACR metric. In addition to the settings discussed in Section 4, we include results for $\alpha \in [0.1, 0.15, 0.2]$ in Table 17.

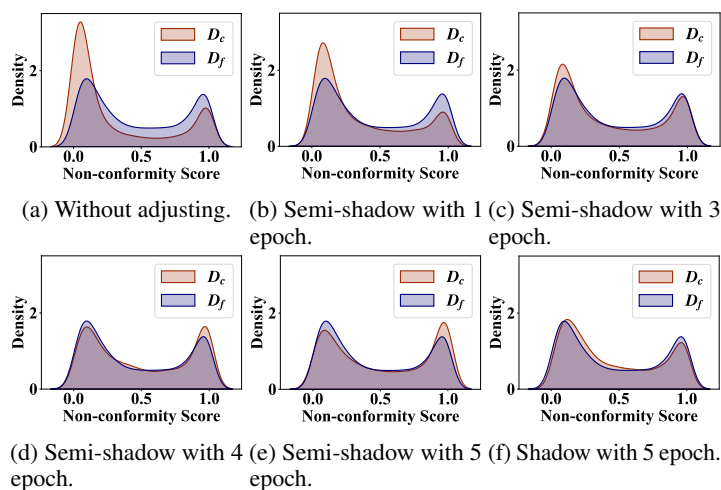


Figure 4: Distribution shifting processing with different strategies. The distribution of calibration data gradually converges with that of forget data.

D.5 MEASURING FORGETTING UNDER DISTRIBUTION SHIFTS

RL and Salun are unlearning methods that employ label corruption in their unlearning strategy, which can cause distribution shifts. Here, we introduce how to better measure forgetting under these circumstances. Figure 4(a) shows the non-conformity score distribution of calibration data \mathcal{D}_c and forget data \mathcal{D}_f in the unlearning model θ_u obtained by the RL method in Tiny ImageNet with ViT. It looks like there is a significant discrepancy between the distribution of the forget data and the calibration data.

To align the distribution of \mathcal{D}_c with that of \mathcal{D}_f and minimize the differences between them, we design a shadow model. To make the explanation clearer and more intuitive, we take RL as an example. In the RL unlearning method, the forget data is assigned random labels. Therefore, we apply the same random labeling process to the calibration data and train a shadow model accordingly. We designed two methods:

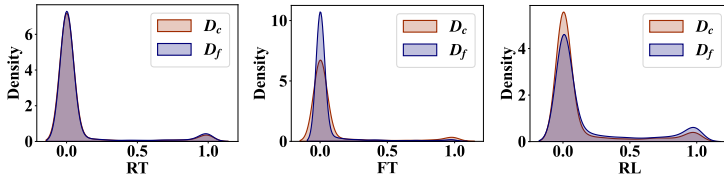


Figure 5: Non-conformity density of calibration data \mathcal{D}_c and forget data \mathcal{D}_f **without our unlearning framework** in CIFAR-10 with ResNet-18 under 10% random data forgetting scenario.

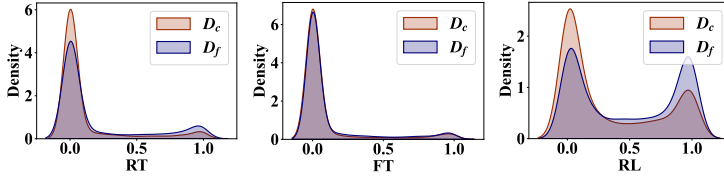


Figure 6: Non-conformity score density of calibration data \mathcal{D}_c and forget data \mathcal{D}_f **with our unlearning framework** in CIFAR-10 with ResNet-18 under 10% random data forgetting scenario. Our unlearning framework shifts the distribution of the forget data to the right, demonstrating improved forgetting quality.

1. **Shadow model.** A shadow model replicates the behavior of forget data \mathcal{D}_f throughout the unlearning process. A shadow model is a two-step approach: (1) it firstly trains a shadow original model θ'_o using train data \mathcal{D}_{train} and clean calibration data \mathcal{D}_c with the same epoch number as the original model θ_o ; (2) subsequently, we finetune the θ'_o using the random labeled calibration data.
2. **Semi-shadow model.** The semi-shadow model only adopts the second step in the shadow model. It finetunes the original model θ_o with random-labeled calibration data.

The results are presented in Figure 4, where (b)-(e) present the results of the semi-shadow model with different epochs and (f) illustrates the shadow model’s result. Under the semi-shadow model, as the number of epochs increases, the distribution of calibration data gradually moves to the right until it becomes consistent with the distribution of forget data. It also shows that the shadow model demonstrates the best ability to handle distribution shifts compared to the semi-shadow model. However, this comes at the cost of higher computational overhead. Overall, the semi-shadow model offers a balanced trade-off between handling distribution shifts effectively and maintaining lower computational costs.

E PERFORMANCE OF OUR UNLEARNING FRAMEWORK

E.1 UNLEARNING PERFORMANCE

Table 18 presents the performance of our unlearning framework, including $\alpha \in [0.05, 0.1, 0.15, 0.2]$. We explored the impact of varying λ within the range $[0, 0.2, 0.5, 0.1]$, where $\lambda = 0$ serves as the baseline without applying our framework, which can be found in Tables 11 and 14. The results reveal a clear trend: as λ increases, the UA improves significantly across all methods, accompanied by a substantial reduction in $CR_{\mathcal{D}_f}$. Interestingly, the RA, TA, and $CRDtest$ metrics remain relatively stable. These results underscore the effectiveness of our unlearning framework in achieving substantial improvements in forgetting quality while preserving the stability of the model’s predictive performance.

Furthermore, we conduct an ablation study and analyze the impact of using our unlearning framework. As illustrated in Figures 5 and 6, we compare the density distributions of non-conformity scores for calibration data \mathcal{D}_c and forget data \mathcal{D}_f under the RT, FT, and RL unlearning methods. We set λ to 1. Clearly, a higher non-conformity score for \mathcal{D}_f indicates that it is less likely to be included in the conformal prediction set, reflecting more effective forgetting.

Comparing Figures 5 and 6, after applying our unlearning framework, we observe a significant rightward shift in the non-conformity score distribution of forget data, which is a promising signal

according to evaluation criterion ②. Furthermore, the FT distribution in Figure 6 exhibits substantial overlap with the calibration data, nearly matching the distribution observed in RT. Based on evaluation criterion ①, since calibration data represents unseen examples, the similarity between forget data and calibration data distributions provides strong evidence of effective forgetting. Overall, the results evaluated on both evaluation criteria ① and ② consistently confirm the efficacy of our framework in enhancing forgetting quality.

Table 7: Training time comparison (in minutes) with and without our CPU loss.

Methods	w/o CPU	w/ CPU
CIFAR-10 with ResNet18		
RT	70.1	72.1
FT	6.3	6.8
RL	6.3	6.8
Tiny ImageNet with ViT		
RT	60.75	62.85
FT	20.2	22.1
RL	21.3	23.4

E.2 TIME COMPARISON

We compare the training time with and without our unlearning calibration process on CIFAR-10 and Tiny ImageNet under the 10% random data forgetting scenario. As shown in Table 7, the training times with and without CPU support differ only marginally, confirming that our CPU loss computation introduces negligible overhead.

F OTHER CONFORMAL PREDICTION METHODS

Table 8: CR performance with different conformal prediction methods. The performance gap relative to the RT method is represented in (•).

Methods	LAC		EntmaxScore		APS	
	CR(\mathcal{D}_f) \downarrow	CR(\mathcal{D}_f) \uparrow	CR(\mathcal{D}_f) \downarrow	CR(\mathcal{D}_f) \uparrow	CR(\mathcal{D}_f) \downarrow	CR(\mathcal{D}_f) \uparrow
RT	0.862(0.000)	0.876(0.000)	0.863(0.000)	0.877(0.000)	0.805(0.000)	0.836(0.000)
FT	0.901(0.039)	0.846(0.030)	0.901(0.038)	0.848(0.029)	0.808(0.004)	0.784(0.052)
RL	0.676(0.186)	0.752(0.124)	0.883(0.020)	0.838(0.039)	0.573(0.232)	0.670(0.166)
GA	0.995(0.133)	0.931(0.055)	0.995(0.132)	0.930(0.054)	0.985(0.180)	0.875(0.038)
Teacher	0.988(0.127)	0.915(0.039)	0.987(0.125)	0.917(0.040)	0.511(0.293)	0.536(0.300)
SSD	0.995(0.133)	0.933(0.057)	0.994(0.131)	0.930(0.054)	0.985(0.181)	0.876(0.039)
NegGrad+	0.865(0.003)	0.863(0.013)	0.869(0.006)	0.870(0.006)	0.860(0.056)	0.856(0.020)
Salun	0.881(0.019)	0.839(0.037)	0.878(0.015)	0.839(0.038)	0.407(0.398)	0.430(0.407)
SFRon	0.893(0.031)	0.838(0.038)	0.893(0.030)	0.838(0.039)	0.815(0.010)	0.769(0.067)

While we adopt vanilla split-conformal as the default due to its simplicity and reproducibility, our framework is not limited to this variant. Here, we report the results using other conformal prediction methods, LAC Sadinle et al. (2019), EntmaxScore Campos et al. (2025), and ASP Romano et al. (2020b) on CIFAR-10 with ResNet18 under 10% random data forgetting.

As shown in the Table 8, the CR results of LAC and EntmaxScore are similar to those obtained using SCP in Table 3. This suggests that the results are stable under conformal prediction methods that offer formal coverage guarantees. However, APS produces different CR values compared to LAC, SCP, and EntmaxScore. This discrepancy is expected and is due to the inherent characteristics of APS, which make it unsuitable for evaluating unlearning metrics. APS generally produces loose prediction sets and is highly sensitive to noisy probability estimates in the lower-ranked classes Angelopoulos et al. (2020), which introduces randomness in the ordering of unlikely classes and leads to unreliable set construction. Our findings indicate that not all conformal prediction methods are inherently suitable for evaluating forgetting quality. And the reliability of such evaluation depends critically on whether the resulting prediction sets faithfully capture the model’s uncertainty.

918 Table 9: Unlearning performance on **CIFAR-10** with **ResNet-18** in **10% worst-case data forgetting**
919 scenario. The results are reported in the format $a \pm b$, where a is the mean and b is the standard
920 deviation from 3 independent trials. The performance gap relative to the RT method is represented in
921 (•).

Methods	Existing Metrics			Coverage		Set Size		CR	
	UA \uparrow	RA \uparrow	TA \uparrow	$\mathcal{D}_f \downarrow$	$\mathcal{D}_{test} \uparrow$	$\mathcal{D}_f \uparrow$	$\mathcal{D}_{test} \downarrow$	$\mathcal{D}_f \downarrow$	$\mathcal{D}_{test} \uparrow$
RT	0.0% (0.0)	99.8% (0.6)	94.1% (2.6)	1.000 (0.000)	0.948 (0.000)	1.000 (0.000)	1.116 (0.000)	1.000 (0.000)	0.850 (0.000)
FT	0.0% (0.0)	99.8% (0.6)	94.1% (2.6)	1.000 (0.000)	0.938 (0.010)	1.000 (0.000)	0.992 (0.124)	1.000 (0.000)	0.945 (0.095)
RL	21.3% (21.3)	97.4% (1.7)	88.5% (3.0)	0.976 (0.024)	0.955 (0.007)	6.753 (5.753)	2.192 (1.076)	0.146 (0.854)	0.441 (0.409)
GA	0.3% (0.3)	96.9% (2.2)	91.3% (0.2)	0.999 (0.001)	0.954 (0.006)	1.029 (0.029)	1.179 (0.063)	0.971 (0.029)	0.810 (0.040)
Teacher	15.8% (15.8)	97.9% (1.2)	90.6% (0.9)	0.850 (0.150)	0.946 (0.002)	1.177 (0.177)	1.249 (0.133)	0.745 (0.255)	0.760 (0.090)
SSD	0.0% (0.0)	99.7% (0.5)	94.0% (2.6)	1.000 (0.000)	0.954 (0.006)	1.000 (0.000)	1.037 (0.079)	1.000 (0.000)	0.920 (0.070)
NegGrad+	0.0% (0.0)	99.8% (0.6)	94.2% (2.7)	1.000 (0.000)	0.947 (0.001)	1.000 (0.000)	1.012 (0.104)	1.000 (0.000)	0.936 (0.086)
SalUn	13.0% (13.0)	97.6% (1.6)	90.0% (1.5)	0.962 (0.038)	0.947 (0.001)	3.991 (2.991)	1.567 (0.451)	0.246 (0.754)	0.606 (0.244)
SFRon	0.0% (0.0)	99.5% (0.3)	93.8% (2.4)	1.000 (0.000)	0.956 (0.008)	1.000 (0.000)	1.053 (0.063)	1.000 (0.000)	0.908 (0.058)

931
932 Overall, conformal prediction serves as a component within our uncertainty quantification-based
933 evaluation framework. The simplest and most straightforward conformal prediction methods, es-
934 pecially SCP, are often the most suitable tools. While many recent conformal prediction variants
935 improve upon different issues, e.g., by modifying the nonconformity scores or explicitly penalizing
936 low-probability classes Angelopoulos et al. (2020); Huang et al. (2023), these techniques often distort
937 the nonconformity values across some classes. Since our goal is to use conformal prediction as a tool
938 for designing fair metrics and evaluating forgetting quality, we intentionally avoid such modifications.
939 Introducing these more complex methods could result in additional noise, thereby compromising the
940 fairness and interpretability of our evaluation.

G OTHER FORGETTING SCENARIO

941
942 **Worst-case Forgetting scenario** Random data forgetting may affect unlearning models differently,
943 introducing variance and bias that make it a relatively weak evaluation setting. To more rigorously
944 assess the effectiveness of our proposed metrics, we further evaluate them using worst-case forget
945 sets Fan et al. (2024a). As shown in Table 9, the results are consistent with our previous analysis.

946 Table 10: Unlearning performance on **CIFAR-20** with **ResNet18** in **subclass-wise forgetting**
947 scenario.

Methods	Existing Metrics			Coverage		Set Size		CR	
	UA \uparrow	UA _{rt} \uparrow	RA \uparrow	$\mathcal{D}_f \downarrow$	$\mathcal{D}_{tr} \uparrow$	$\mathcal{D}_f \uparrow$	$\mathcal{D}_{tr} \downarrow$	$\mathcal{D}_f \downarrow$	$\mathcal{D}_{tr} \uparrow$
RT	97.6% (0.0)	94.0% (0.0)	99.9% (0.0)	84.5% (0.0)	1.000 (0.000)	1.000 (0.000)	0.953 (0.000)	20.000 (0.300)	17.713 (0.000)
FT	70.9% (30.7)	74.7% (19.3)	95.7% (1.1)	76.0% (6.6)	0.994 (0.006)	0.987 (0.013)	0.952 (0.001)	17.637 (2.363)	16.893 (3.167)
RL	99.5% (1.0)	94.7% (0.7)	98.2% (1.7)	76.7% (7.0)	0.931 (0.000)	1.000 (0.000)	0.955 (0.001)	18.897 (1.193)	19.537 (0.473)
GA	40.7% (56.9)	60.7% (33.3)	99.0% (0.8)	82.2% (2.3)	0.999 (0.001)	0.993 (0.007)	0.954 (0.001)	18.305 (1.695)	17.553 (2.447)
Teacher	90.6% (7.0)	97.3% (3.3)	98.6% (1.3)	81.3% (3.2)	0.989 (0.011)	0.933 (0.067)	0.948 (0.005)	19.871 (0.129)	18.840 (1.160)
SSD	73.6% (24.0)	80.0% (14.0)	99.8% (0.0)	84.5% (0.0)	0.997 (0.003)	0.980 (0.020)	0.955 (0.001)	19.206 (0.794)	17.740 (2.260)
NegGrad+	98.9% (1.3)	100.0% (6.0)	97.0% (2.8)	80.9% (3.7)	1.000 (0.000)	1.000 (0.000)	0.950 (0.003)	20.000 (0.000)	20.000 (0.000)
SalUn	99.9% (2.3)	96.0% (2.0)	98.8% (1.0)	78.9% (5.6)	0.955 (0.045)	0.993 (0.007)	0.951 (0.002)	19.235 (0.765)	19.707 (0.293)
SFRon	99.9% (2.3)	100.0% (6.0)	91.9% (7.9)	79.7% (4.9)	1.000 (0.000)	0.951 (0.003)	20.000 (0.000)	20.000 (0.000)	2.587 (0.874)

948
949 **Subclass-wise Forgetting Scenario** To further verify our metrics in other forgetting scenarios, we
950 report subclass-wise forgetting results on CIFAR-20 (derived from CIFAR-100) using ResNet-18,
951 following the setting proposed in Foster et al. (2024). As shown in the Table 10, the findings align
952 well with our prior analysis.

H LARGE LANGUAGE MODELS USAGE STATEMENT

953
954 We used a large language model (LLM) to polish the language and improve the clarity of the paper.
955 All content, including the core ideas, methodology, and experimental results, was originally created by
956 the authors. The LLM was used exclusively as an editing tool to enhance readability and grammatical
957 correctness, without generating any substantive or technical content.

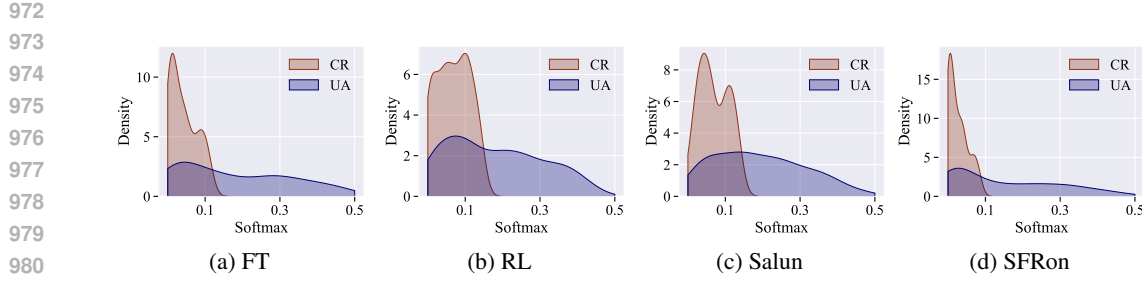


Figure 7: **Softmax distribution in 10% random data forgetting** scenario. We analyze the softmax distributions of true labels for data identified as truly forgotten by CR and UA, respectively. The distribution curves are fitted using KDE for clearer visualization. The results illustrate the softmax distributions of CR consistently closer to 0 when compared to UA, providing strong evidence that CR is better than UA in accurately capturing and measuring ‘real forgetting’.

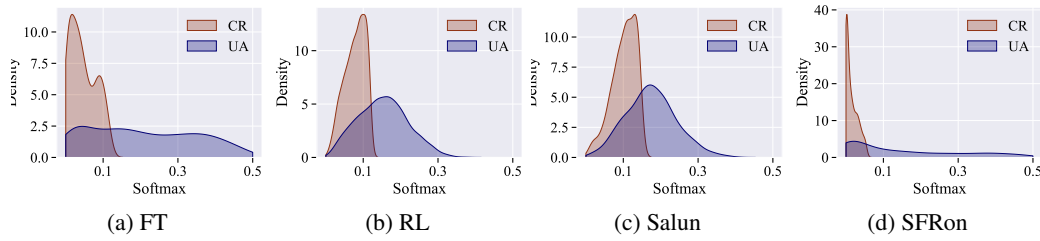


Figure 8: **Softmax distribution in 50% random data forgetting** scenario.

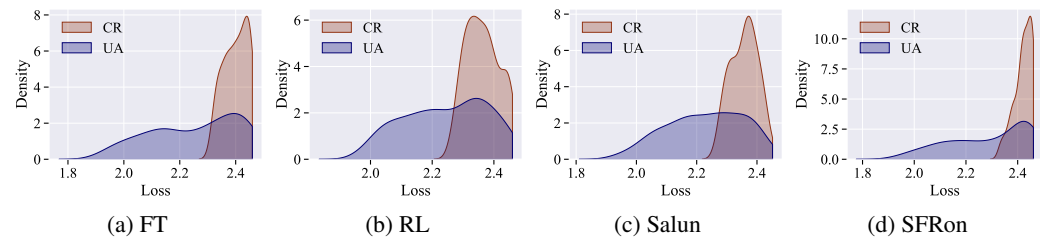


Figure 9: **Loss distribution in 10% random data forgetting** scenario. We analyze the cross-entropy loss distributions of true labels for data identified as truly forgotten by CR and UA, respectively. Forgotten data identified by CR consistently show higher cross-entropy loss than UA. Higher loss indicates better forgetting quality, which further validates that CR better captures ‘real forgetting’.

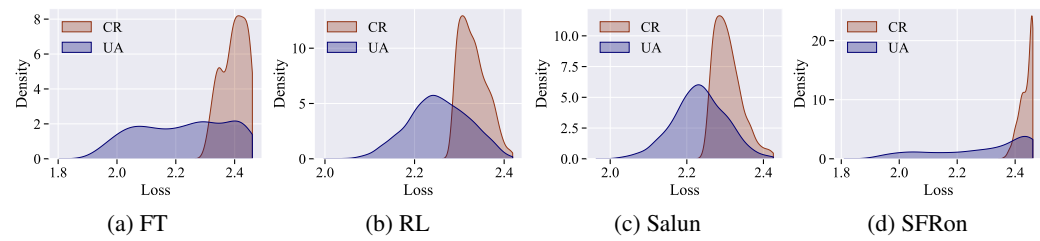


Figure 10: **Loss distribution in 50% random data forgetting** scenario.

1026

1027

1028
1029
1030
1031
Table 11: Unlearning performance of 9 unlearning methods on **CIFAR-10** with **ResNet-18** in **10% random data forgetting** scenario. The results are reported in the format $a \pm b$, where a is the mean and b is the standard deviation from 3 independent trials. The performance gap relative to the RT method is represented in (\bullet) .

Methods	α	Coverage		Set Size		CR		\hat{q}
		$\mathcal{D}_f \downarrow$	$\mathcal{D}_{test} \uparrow$	$\mathcal{D}_f \uparrow$	$\mathcal{D}_{test} \downarrow$	$\mathcal{D}_f \downarrow$	$\mathcal{D}_{test} \uparrow$	
RT	0.05	0.941 \pm 0.002 (0.000)	0.944 \pm 0.005 (0.000)	1.089 \pm 0.002 (0.000)	1.074 \pm 0.011 (0.000)	0.864 \pm 0.004 (0.000)	0.879 \pm 0.004 (0.000)	0.883 \pm 0.007
	0.1	0.881 \pm 0.000 (0.000)	0.895 \pm 0.010 (0.000)	0.934 \pm 0.004 (0.000)	0.947 \pm 0.008 (0.000)	0.943 \pm 0.011 (0.000)	0.945 \pm 0.001 (0.000)	0.192 \pm 0.001
	0.15	0.820 \pm 0.002 (0.000)	0.839 \pm 0.008 (0.000)	0.841 \pm 0.009 (0.000)	0.867 \pm 0.009 (0.000)	0.975 \pm 0.001 (0.000)	0.968 \pm 0.003 (0.000)	0.015 \pm 0.011
	0.2	0.780 \pm 0.007 (0.000)	0.808 \pm 0.004 (0.000)	0.789 \pm 0.002 (0.000)	0.824 \pm 0.009 (0.000)	0.988 \pm 0.006 (0.000)	0.981 \pm 0.007 (0.000)	0.003 \pm 0.002
FT	0.05	0.994 \pm 0.001 (0.053)	0.951 \pm 0.004 (0.007)	1.008 \pm 0.003 (0.081)	1.026 \pm 0.008 (0.048)	0.986 \pm 0.003 (0.122)	0.927 \pm 0.004 (0.048)	0.721 \pm 0.045
	0.1	0.968 \pm 0.001 (0.087)	0.899 \pm 0.005 (0.004)	0.969 \pm 0.001 (0.035)	0.924 \pm 0.008 (0.023)	0.998 \pm 0.001 (0.055)	0.972 \pm 0.003 (0.027)	0.079 \pm 0.013
	0.15	0.915 \pm 0.003 (0.095)	0.848 \pm 0.003 (0.004)	0.916 \pm 0.003 (0.075)	0.860 \pm 0.001 (0.007)	1.000 \pm 0.000 (0.025)	0.986 \pm 0.002 (0.018)	0.008 \pm 0.000
	0.2	0.861 \pm 0.010 (0.081)	0.806 \pm 0.008 (0.002)	0.861 \pm 0.010 (0.072)	0.811 \pm 0.009 (0.013)	1.000 \pm 0.000 (0.012)	0.993 \pm 0.001 (0.012)	0.002 \pm 0.000
RL	0.05	0.970 \pm 0.006 (0.029)	0.949 \pm 0.005 (0.005)	1.242 \pm 0.151 (0.153)	1.197 \pm 0.098 (0.123)	0.788 \pm 0.089 (0.076)	0.796 \pm 0.061 (0.083)	0.877 \pm 0.057
	0.1	0.913 \pm 0.010 (0.032)	0.897 \pm 0.007 (0.002)	0.975 \pm 0.028 (0.041)	0.980 \pm 0.025 (0.033)	0.936 \pm 0.022 (0.007)	0.918 \pm 0.019 (0.029)	0.572 \pm 0.059
	0.15	0.825 \pm 0.006 (0.005)	0.843 \pm 0.009 (0.004)	0.854 \pm 0.010 (0.013)	0.885 \pm 0.017 (0.021)	0.960 \pm 0.006 (0.009)	0.949 \pm 0.009 (0.019)	0.329 \pm 0.021
	0.2	0.755 \pm 0.021 (0.025)	0.798 \pm 0.005 (0.010)	0.774 \pm 0.020 (0.015)	0.832 \pm 0.009 (0.008)	0.976 \pm 0.002 (0.012)	0.959 \pm 0.005 (0.022)	0.234 \pm 0.028
GA	0.05	0.994 \pm 0.003 (0.053)	0.945 \pm 0.008 (0.001)	1.002 \pm 0.010 (0.087)	1.009 \pm 0.010 (0.065)	0.994 \pm 0.016 (0.130)	0.936 \pm 0.011 (0.057)	0.621 \pm 0.015
	0.1	0.990 \pm 0.001 (0.109)	0.905 \pm 0.019 (0.010)	0.990 \pm 0.014 (0.056)	0.928 \pm 0.005 (0.019)	0.998 \pm 0.002 (0.055)	0.973 \pm 0.012 (0.028)	0.062 \pm 0.016
	0.15	0.969 \pm 0.012 (0.149)	0.848 \pm 0.004 (0.009)	0.969 \pm 0.014 (0.128)	0.858 \pm 0.019 (0.009)	1.000 \pm 0.014 (0.025)	0.986 \pm 0.008 (0.018)	0.006 \pm 0.009
	0.2	0.925 \pm 0.012 (0.145)	0.805 \pm 0.022 (0.003)	0.924 \pm 0.007 (0.135)	0.811 \pm 0.013 (0.013)	0.998 \pm 0.013 (0.010)	0.992 \pm 0.012 (0.011)	0.003 \pm 0.005
Teacher	0.05	0.991 \pm 0.022 (0.050)	0.941 \pm 0.001 (0.003)	1.003 \pm 0.012 (0.086)	1.021 \pm 0.009 (0.053)	0.993 \pm 0.021 (0.129)	0.922 \pm 0.015 (0.043)	0.744 \pm 0.015
	0.1	0.967 \pm 0.000 (0.086)	0.898 \pm 0.007 (0.003)	0.963 \pm 0.007 (0.029)	0.929 \pm 0.018 (0.018)	0.998 \pm 0.000 (0.055)	0.969 \pm 0.013 (0.024)	0.591 \pm 0.005
	0.15	0.913 \pm 0.006 (0.093)	0.845 \pm 0.007 (0.006)	0.912 \pm 0.014 (0.071)	0.859 \pm 0.005 (0.008)	0.996 \pm 0.018 (0.021)	0.983 \pm 0.015 (0.015)	0.481 \pm 0.009
	0.2	0.865 \pm 0.009 (0.085)	0.806 \pm 0.021 (0.002)	0.866 \pm 0.009 (0.077)	0.816 \pm 0.012 (0.008)	0.998 \pm 0.008 (0.010)	0.988 \pm 0.016 (0.007)	0.426 \pm 0.007
SSD	0.05	0.996 \pm 0.004 (0.055)	0.945 \pm 0.002 (0.001)	0.999 \pm 0.019 (0.090)	1.008 \pm 0.011 (0.066)	0.994 \pm 0.006 (0.130)	0.936 \pm 0.014 (0.057)	0.622 \pm 0.019
	0.1	0.987 \pm 0.003 (0.062)	0.902 \pm 0.010 (0.007)	0.990 \pm 0.003 (0.056)	0.926 \pm 0.017 (0.021)	0.998 \pm 0.020 (0.055)	0.973 \pm 0.002 (0.028)	0.063 \pm 0.022
	0.15	0.967 \pm 0.016 (0.147)	0.849 \pm 0.009 (0.010)	0.965 \pm 0.000 (0.124)	0.862 \pm 0.012 (0.005)	1.002 \pm 0.019 (0.027)	0.990 \pm 0.002 (0.022)	0.007 \pm 0.007
	0.2	0.922 \pm 0.006 (0.142)	0.803 \pm 0.004 (0.005)	0.923 \pm 0.009 (0.134)	0.811 \pm 0.005 (0.013)	1.002 \pm 0.020 (0.014)	0.992 \pm 0.009 (0.011)	0.001 \pm 0.005
NegGrad+	0.05	0.934 \pm 0.007 (0.007)	0.948 \pm 0.007 (0.004)	1.068 \pm 0.017 (0.021)	1.086 \pm 0.022 (0.012)	0.875 \pm 0.008 (0.011)	0.873 \pm 0.011 (0.006)	0.989 \pm 0.013
	0.1	0.895 \pm 0.004 (0.014)	0.898 \pm 0.008 (0.003)	0.964 \pm 0.008 (0.030)	0.950 \pm 0.013 (0.003)	0.928 \pm 0.005 (0.015)	0.946 \pm 0.005 (0.001)	0.044 \pm 0.041
	0.15	0.851 \pm 0.013 (0.031)	0.851 \pm 0.016 (0.012)	0.896 \pm 0.016 (0.055)	0.876 \pm 0.019 (0.009)	0.950 \pm 0.003 (0.025)	0.971 \pm 0.003 (0.003)	0.000 \pm 0.000
	0.2	0.800 \pm 0.006 (0.020)	0.799 \pm 0.001 (0.009)	0.832 \pm 0.006 (0.043)	0.813 \pm 0.001 (0.011)	0.961 \pm 0.002 (0.027)	0.983 \pm 0.001 (0.002)	0.000 \pm 0.000
Salun	0.05	0.987 \pm 0.002 (0.046)	0.950 \pm 0.001 (0.006)	1.132 \pm 0.007 (0.043)	1.143 \pm 0.002 (0.069)	0.872 \pm 0.006 (0.008)	0.832 \pm 0.003 (0.047)	0.867 \pm 0.001
	0.1	0.936 \pm 0.010 (0.055)	0.896 \pm 0.008 (0.001)	0.956 \pm 0.012 (0.022)	0.954 \pm 0.011 (0.007)	0.979 \pm 0.003 (0.036)	0.939 \pm 0.003 (0.006)	0.489 \pm 0.029
	0.15	0.871 \pm 0.005 (0.051)	0.849 \pm 0.008 (0.010)	0.881 \pm 0.006 (0.040)	0.886 \pm 0.016 (0.010)	0.989 \pm 0.002 (0.014)	0.955 \pm 0.002 (0.010)	0.314 \pm 0.020
	0.2	0.788 \pm 0.005 (0.048)	0.794 \pm 0.001 (0.014)	0.794 \pm 0.010 (0.049)	0.821 \pm 0.004 (0.003)	0.992 \pm 0.001 (0.004)	0.966 \pm 0.003 (0.015)	0.221 \pm 0.005
SFRon	0.05	0.977 \pm 0.003 (0.036)	0.953 \pm 0.004 (0.009)	1.100 \pm 0.023 (0.011)	1.143 \pm 0.021 (0.069)	0.889 \pm 0.015 (0.025)	0.834 \pm 0.012 (0.045)	0.926 \pm 0.018
	0.1	0.945 \pm 0.004 (0.064)	0.905 \pm 0.005 (0.010)	0.986 \pm 0.005 (0.052)	0.977 \pm 0.008 (0.030)	0.958 \pm 0.001 (0.015)	0.927 \pm 0.003 (0.018)	0.435 \pm 0.043
	0.15	0.895 \pm 0.002 (0.075)	0.847 \pm 0.002 (0.008)	0.912 \pm 0.004 (0.071)	0.879 \pm 0.001 (0.012)	0.982 \pm 0.002 (0.007)	0.963 \pm 0.003 (0.005)	0.082 \pm 0.007
	0.2	0.857 \pm 0.008 (0.077)	0.808 \pm 0.002 (0.000)	0.868 \pm 0.007 (0.079)	0.826 \pm 0.005 (0.002)	0.988 \pm 0.002 (0.000)	0.978 \pm 0.004 (0.003)	0.025 \pm 0.005
GA	0.05	0.985 \pm 0.015 (0.030)	0.944 \pm 0.012 (0.003)	1.066 \pm 0.003 (0.021)	1.143 \pm 0.012 (0.071)	0.923 \pm 0.010 (0.181)	0.823 \pm 0.017 (0.043)	0.857 \pm 0.013
	0.1	0.949 \pm 0.012 (0.051)	0.909 \pm 0.016 (0.005)	0.970 \pm 0.006 (0.035)	0.986 \pm 0.014 (0.035)	0.980 \pm 0.001 (0.102)	0.918 \pm 0.009 (0.032)	0.834 \pm 0.005
	0.15	0.885 \pm 0.010 (0.052)	0.849 \pm 0.015 (0.002)	0.894 \pm 0.017 (0.011)	0.893 \pm 0.010 (0.013)	0.950 \pm 0.013 (0.016)	0.813 \pm 0.013 (0.012)	0.000 \pm 0.000
	0.2	0.818 \pm 0.014 (0.036)	0.798 \pm 0.014 (0.016)	0.823 \pm 0.006 (0.011)	0.826 \pm 0.002 (0.024)	0.997 \pm 0.015 (0.033)	0.971 \pm 0.007 (0.013)	0.793 \pm 0.012
SSD	0.05	0.993 \pm 0.005 (0.038)	0.944 \pm 0.011 (0.003)	1.003 \pm 0.007 (0.084)	1.024 \pm 0.009 (0.213)	1.001 \pm 0.009 (0.213)	0.995 \pm 0.009 (0.253)	0.941 \pm 0.013 (0.161)
	0.1	0.991 \pm 0.011 (0.039)	0.904 \pm 0.014 (0.000)	0.991 \pm 0.001 (0.032)	0.929 \pm 0.001 (0.092)	1.002 \pm 0.012 (0.122)	0.975 \pm 0.010 (0.089)	0.060 \pm 0.011
	0.15	0.964 \pm 0.016 (0.131)	0.850 \pm 0.011 (0.003)	0.967 \pm 0.006 (0.084)	0.860 \pm 0.014 (0.046)	1.000 \pm 0.001 (0.057)	0.985 \pm 0.003 (0.054)	0.005 \pm 0.010
	0.2	0.930 \pm 0.018 (0.148)	0.807 \pm 0.002 (0.007)	0.929 \pm 0.002 (0.117)	0.814 \pm 0.017 (0.036)	1.000 \pm 0.003 (0.036)	0.992 \pm 0.001 (0.034)	0.002 \pm 0.005
NegGrad+	0.05	0.986 \pm 0.000 (0.031)	0.949 \pm 0.001 (0.001)	1.039 \pm 0.008 (0.248)	1.062 \pm 0.011 (0.152)	0.949 \pm 0.008 (0.207)	0.893 \pm 0.008 (0.113)	0.855 \pm 0.028
	0.1	0.951 \pm 0.005 (0.053)	0.903 \pm 0.004 (0.001)	0.964 \pm 0.006 (0.059)	0.944 \pm 0.010 (0.076)	0.987 \pm 0.003 (0.109)	0.956 \pm 0.007 (0.070)	0.177 \pm 0.055
	0.15	0.889 \pm 0.004 (0.056)	0.845 \pm 0.003 (0.002)	0.892 \pm 0.004 (0.049)	0.861 \pm 0.003 (0.045)	0.996 \pm 0.003 (0.053)	0.981 \pm 0.001 (0.047)	0.012 \pm 0.002
	0.2	0.825 \pm 0.003 (0.043)	0.796 \pm 0.001 (0.018)	0.827 \pm 0.003 (0.015)	0.805 \pm 0.004 (0.045)	0.999 \pm 0.000 (0.035)	0.989 \pm 0.000 (0.032)	0.002 \pm 0.000
Salun	0.05	0.988 \pm 0.001 (0.034)	0.951 \pm 0.003 (0.004)	1.314 \pm 0.113 (0.027)	1.381 \pm 0.121 (0.167)	0.756 \pm 0.064 (0.014)	0.692 \pm 0.058 (0.088)	0.871 \pm 0.013

1080
1081
1082
1083
1084
1085Table 13: Unlearning performance of 9 unlearning methods on **CIFAR-10** with **ResNet18** in **class-wise forgetting** scenario.

Methods	α	Coverage		Set Size		CR		\hat{q}_f	\hat{q}_{test}	
		$D_f \downarrow$	$D_{te} \uparrow$	$D_f \uparrow$	$D_{te} \downarrow$	$D_f \downarrow$	$D_{te} \uparrow$			
RT	0.05	1.000 \pm 0.000 (0.000)	1.000 \pm 0.001 (0.000)	0.964 \pm 0.008 (0.000)	10.000 \pm 0.000 (0.000)	10.000 \pm 0.000 (0.000)	1.148 \pm 0.013 (0.000)	1.100 \pm 0.000 (0.000)	1.100 \pm 0.000 (0.000)	0.840 \pm 0.002 (0.000)
UA100%, UA \downarrow 100%, RA99.5%, TA92.4%	0.1	1.000 \pm 0.000 (0.000)	1.000 \pm 0.001 (0.000)	0.889 \pm 0.011 (0.000)	10.000 \pm 0.000 (0.000)	10.000 \pm 0.000 (0.000)	0.922 \pm 0.000 (0.000)	0.100 \pm 0.000 (0.000)	0.100 \pm 0.000 (0.000)	0.956 \pm 0.000 (0.000)
FT	0.05	0.994 \pm 0.000 (0.000)	0.962 \pm 0.002 (0.038)	0.944 \pm 0.011 (0.020)	9.854 \pm 0.010 (0.116)	4.033 \pm 0.010 (0.597)	1.045 \pm 0.000 (0.103)	1.011 \pm 0.001 (0.001)	1.012 \pm 0.000 (0.002)	0.904 \pm 0.000 (0.005)
UA100%, UA \downarrow 100%, RA96.7%, TA90.8%	0.1	0.969 \pm 0.011 (0.031)	0.882 \pm 0.020 (0.118)	0.908 \pm 0.010 (0.026)	9.405 \pm 0.020 (0.105)	8.528 \pm 0.171 (1.472)	0.956 \pm 0.008 (0.034)	0.102 \pm 0.002 (0.002)	0.104 \pm 0.002 (0.004)	0.950 \pm 0.000 (0.006)
RL	0.05	0.994 \pm 0.000 (0.000)	0.962 \pm 0.002 (0.038)	0.944 \pm 0.011 (0.020)	9.854 \pm 0.010 (0.116)	4.033 \pm 0.010 (0.597)	1.045 \pm 0.000 (0.103)	1.011 \pm 0.001 (0.001)	1.012 \pm 0.000 (0.002)	0.904 \pm 0.000 (0.005)
UA100%, UA \downarrow 100%, RA95.0%, TA92.7%	0.1	0.964 \pm 0.011 (0.030)	0.881 \pm 0.020 (0.119)	0.818 \pm 0.010 (0.025)	9.265 \pm 0.020 (0.105)	8.131 \pm 0.321 (1.869)	0.872 \pm 0.009 (0.031)	0.103 \pm 0.003 (0.003)	0.105 \pm 0.003 (0.003)	0.976 \pm 0.000 (0.006)
GA	0.05	1.000 \pm 0.000 (0.000)	1.000 \pm 0.000 (0.000)	0.915 \pm 0.012 (0.036)	9.993 \pm 0.000 (0.005)	9.978 \pm 0.010 (0.022)	9.809 \pm 0.010 (0.020)	0.982 \pm 0.000 (0.009)	0.999 \pm 0.000 (0.001)	0.994 \pm 0.002 (0.007)
UA84.6%, UA \downarrow 82.5%, RA96.4%, TA89.6%	0.1	1.000 \pm 0.000 (0.000)	1.000 \pm 0.001 (0.000)	0.842 \pm 0.011 (0.013)	10.000 \pm 0.000 (0.000)	10.000 \pm 0.000 (0.000)	0.893 \pm 0.010 (0.011)	0.100 \pm 0.004 (0.000)	0.100 \pm 0.008 (0.009)	0.944 \pm 0.000 (0.028)
Teacher	0.05	0.994 \pm 0.000 (0.000)	0.959 \pm 0.002 (0.041)	0.939 \pm 0.005 (0.025)	9.877 \pm 0.000 (0.123)	9.502 \pm 0.003 (0.498)	1.000 \pm 0.004 (0.148)	0.101 \pm 0.004 (0.001)	0.101 \pm 0.004 (0.001)	0.939 \pm 0.000 (0.099)
UA90.1%, UA \downarrow 86.5%, RA95.5%, TA94.0%	0.15	0.879 \pm 0.009 (0.121)	0.881 \pm 0.010 (0.119)	0.834 \pm 0.010 (0.022)	8.730 \pm 0.007 (0.216)	8.081 \pm 0.011 (1.319)	0.845 \pm 0.007 (0.037)	0.101 \pm 0.003 (0.001)	0.109 \pm 0.003 (0.009)	0.986 \pm 0.000 (0.016)
SSD	0.05	0.995 \pm 0.004 (0.005)	0.935 \pm 0.009 (0.055)	0.904 \pm 0.014 (0.010)	9.919 \pm 0.008 (0.081)	9.637 \pm 0.008 (0.363)	0.820 \pm 0.008 (0.010)	0.094 \pm 0.002 (0.006)	0.085 \pm 0.002 (0.015)	0.981 \pm 0.002 (0.000)
NegGrad+	0.05	0.989 \pm 0.000 (0.01)	0.961 \pm 0.000 (0.029)	0.949 \pm 0.000 (0.010)	9.432 \pm 0.000 (0.568)	0.000 \pm 0.000 (0.002)	0.000 \pm 0.000 (0.002)	0.100 \pm 0.007 (0.000)	0.100 \pm 0.011 (0.000)	0.988 \pm 0.000 (0.000)
NegGrad+, UA \downarrow 92.5%, RA96.2%	0.15	0.952 \pm 0.000 (0.043)	0.908 \pm 0.001 (0.092)	0.849 \pm 0.008 (0.007)	8.600 \pm 0.000 (1.400)	8.077 \pm 0.211 (1.923)	0.868 \pm 0.016 (0.014)	0.113 \pm 0.013 (0.013)	0.116 \pm 0.023 (0.016)	0.977 \pm 0.002 (0.007)
SRon	0.05	0.998 \pm 0.000 (0.001)	0.941 \pm 0.008 (0.059)	0.952 \pm 0.001 (0.012)	9.996 \pm 0.000 (0.004)	9.892 \pm 0.003 (0.108)	1.028 \pm 0.000 (0.121)	0.100 \pm 0.000 (0.000)	0.095 \pm 0.001 (0.005)	0.926 \pm 0.000 (0.087)
UA100%, UA \downarrow 99%, RA95.6%, TA94.3%	0.15	0.960 \pm 0.002 (0.049)	0.876 \pm 0.011 (0.124)	0.847 \pm 0.007 (0.009)	9.962 \pm 0.000 (0.030)	0.931 \pm 0.006 (0.069)	0.857 \pm 0.013 (0.026)	0.098 \pm 0.008 (0.089)	0.941 \pm 0.002 (0.041)	0.989 \pm 0.000 (0.015)
SSD	0.05	0.995 \pm 0.004 (0.005)	0.935 \pm 0.009 (0.055)	0.904 \pm 0.014 (0.007)	9.862 \pm 0.000 (0.019)	9.862 \pm 0.000 (0.019)	0.994 \pm 0.000 (0.004)	0.099 \pm 0.001 (0.001)	0.099 \pm 0.001 (0.001)	0.994 \pm 0.000 (0.000)
Salun	0.05	0.996 \pm 0.000 (0.001)	0.941 \pm 0.008 (0.059)	0.952 \pm 0.001 (0.012)	9.996 \pm 0.000 (0.004)	9.892 \pm 0.003 (0.108)	1.028 \pm 0.000 (0.121)	0.100 \pm 0.000 (0.000)	0.095 \pm 0.001 (0.005)	0.926 \pm 0.000 (0.089)
UA100%, UA \downarrow 99%, RA95.6%, TA94.3%	0.15	0.960 \pm 0.002 (0.012)	0.881 \pm 0.011 (0.051)	0.878 \pm 0.008 (0.020)	9.981 \pm 0.000 (0.015)	9.817 \pm 0.004 (0.183)	0.905 \pm 0.000 (0.006)	0.100 \pm 0.002 (0.008)	0.097 \pm 0.002 (0.015)	0.971 \pm 0.000 (0.001)
Teacher	0.05	0.997 \pm 0.000 (0.003)	0.956 \pm 0.003 (0.007)	0.947 \pm 0.002 (0.002)	9.573 \pm 0.006 (16.014)	8.572 \pm 0.006 (6.732)	0.054 \pm 0.013 (0.449)	0.111 \pm 0.002 (0.405)	0.111 \pm 0.002 (0.405)	0.996 \pm 0.000 (0.019)
UA17.3%, RA96.0%, TA81.4%	0.15	0.793 \pm 0.021 (0.048)	0.855 \pm 0.008 (0.005)	1.225 \pm 0.013 (0.269)	1.164 \pm 0.006 (0.208)	0.648 \pm 0.002 (0.232)	0.116 \pm 0.006 (0.000)	0.820 \pm 0.022 (0.114)	0.849 \pm 0.006 (0.086)	0.715 \pm 0.013
GA	0.05	0.996 \pm 0.021 (0.025)	0.952 \pm 0.008 (0.003)	2.133 \pm 0.008 (0.257)	2.440 \pm 0.011 (0.600)	0.466 \pm 0.009 (0.037)	0.389 \pm 0.016 (0.127)	0.994 \pm 0.020		
UA3.2%, RA97.4%, TA84.9%	0.15	0.967 \pm 0.002 (0.126)	0.852 \pm 0.005 (0.002)	1.003 \pm 0.008 (0.047)	1.224 \pm 0.002 (0.080)	0.894 \pm 0.004 (0.119)	0.736 \pm 0.006 (0.050)	0.859 \pm 0.006 (0.030)	0.632 \pm 0.009	
Teacher	0.05	0.997 \pm 0.000 (0.003)	0.956 \pm 0.003 (0.007)	5.473 \pm 0.006 (3.597)	5.080 \pm 0.004 (3.240)	2.108 \pm 0.008 (0.178)	0.647 \pm 0.003 (0.144)	0.469 \pm 0.002 (0.047)	0.988 \pm 0.004	
UA17.3%, RA86.7%, TA79.0%	0.15	0.983 \pm 0.003 (0.028)	0.850 \pm 0.009 (0.009)	1.295 \pm 0.006 (0.339)	1.319 \pm 0.006 (0.363)	0.674 \pm 0.007 (0.206)	0.645 \pm 0.003 (0.244)	0.944 \pm 0.006		
SSD	0.05	0.998 \pm 0.004 (0.004)	0.950 \pm 0.006 (0.001)	1.354 \pm 0.008 (0.522)	1.827 \pm 0.002 (0.013)	0.737 \pm 0.008 (0.234)	0.520 \pm 0.008 (0.004)	0.985 \pm 0.005		
UA1.5%, RA98.5%, TA86.1%	0.15	0.958 \pm 0.001 (0.032)	0.853 \pm 0.001 (0.003)	0.993 \pm 0.001 (0.037)	0.962 \pm 0.006 (0.006)	0.988 \pm 0.004 (0.108)	0.887 \pm 0.004 (0.002)	0.542 \pm 0.007		
NegGrad+	0.05	0.999 \pm 0.000 (0.146)	0.890 \pm 0.002 (0.030)	0.949 \pm 0.002 (0.005)	1.614 \pm 0.022 (0.665)	1.052 \pm 0.002 (0.823)	0.552 \pm 0.007 (1.289)	0.995 \pm 0.000		
UA19.4%, RA98.3%, TA84.0%	0.15	0.987 \pm 0.000 (0.137)	0.814 \pm 0.001 (0.047)	0.850 \pm 0.001 (0.009)	1.009 \pm 0.006 (0.159)	1.161 \pm 0.001 (0.206)	0.807 \pm 0.002 (0.149)	0.683 \pm 0.002		
Salun	0.05	0.995 \pm 0.003 (0.142)	0.964 \pm 0.026 (0.103)	2.803 \pm 1.607 (1.859)	2.726 \pm 0.727 (1.777)	0.528 \pm 0.454 (1.347)	0.376 \pm 0.129 (1.464)	0.988 \pm 0.001		
UA9.2%, RA97.7%, TA83.6%	0.15	0.977 \pm 0.014 (0.126)	0.924 \pm 0.040 (0.064)	1.239 \pm 0.286 (0.337)	1.281 \pm 0.120 (0.381)	0.831 \pm 0.237 (0.319)	0.728 \pm 0.104 (0.417)	0.939 \pm 0.005		
SRon	0.05	0.989 \pm 0.001 (0.045)	0.948 \pm 0.001 (0.001)	2.000 \pm 0.050 (0.124)	2.208 \pm 0.037 (0.368)	0.495 \pm 0.014 (0.008)	0.429 \pm 0.007 (0.086)	0.986 \pm 0.000		
UA9.3%, RA97.0%, TA83.9%	0.15	0.917 \pm 0.002 (0.076)	0.849 \pm 0.002 (0.001)	1.024 \pm 0.006 (0.068)	1.015 \pm 0.005 (0.059)	0.896 \pm 0.007 (0.016)	0.837 \pm 0.004 (0.053)	0.689 \pm 0.012		
Salun	0.05	0.995 \pm 0.003 (0.142)	0.964 \pm 0.026 (0.103)	0.916 \pm 0.004 (0.070)	0.802 \pm 0.002 (0.174)	0.972 \pm 0.006 (0.173)	1.205 \pm 0.004 (0.359)	0.805 \pm 0.003 (0.049)	0.320 \pm 0.001	
UA9.3%, RA97.0%, TA83.9%	0.15	0.917 \pm 0.002 (0.076)	0.849 \pm 0.002 (0.001)	1.024 \pm 0.006 (0.068)	1.015 \pm 0.005 (0.059)	0.892 \pm 0.005 (0.037)	0.946 \pm 0.002 (0.012)	0.899 \pm 0.003 (0.036)	0.426 \pm 0.018	

1131
1132
1133

1134
1135
1136
1137
1138
1139

Table 15: Unlearning performance of 9 unlearning methods on Tiny ImageNet with ViT in 50% random data forgetting scenario.

Methods	α	Coverage		Set Size		CR		\hat{q}
		$\mathcal{D}_f \downarrow$	$\mathcal{D}_{test} \uparrow$	$\mathcal{D}_f \uparrow$	$\mathcal{D}_{test} \downarrow$	$\mathcal{D}_f \downarrow$	$\mathcal{D}_{test} \uparrow$	
RT	0.05	0.946 \pm 0.001 (0.000)	0.948 \pm 0.003 (0.000)	2.146 \pm 0.006 (0.000)	2.106 \pm 0.002 (0.000)	0.441 \pm 0.004 (0.000)	0.450 \pm 0.005 (0.000)	0.987 \pm 0.004
	0.1	0.892 \pm 0.007 (0.000)	0.890 \pm 0.008 (0.000)	1.222 \pm 0.002 (0.000)	1.211 \pm 0.007 (0.000)	0.730 \pm 0.004 (0.000)	0.742 \pm 0.002 (0.000)	0.889 \pm 0.009
	0.15	0.838 \pm 0.004 (0.000)	0.847 \pm 0.001 (0.000)	0.977 \pm 0.002 (0.000)	0.977 \pm 0.006 (0.000)	0.858 \pm 0.008 (0.000)	0.868 \pm 0.006 (0.000)	0.607 \pm 0.001
UAI6.0%, RA98.8%, TA84.9%	0.2	0.786 \pm 0.005 (0.000)	0.796 \pm 0.002 (0.000)	0.850 \pm 0.007 (0.000)	0.918 \pm 0.007 (0.000)	0.918 \pm 0.007 (0.000)	0.922 \pm 0.008 (0.000)	0.304 \pm 0.008
FT	0.05	0.995 \pm 0.013 (0.051)	0.949 \pm 0.024 (0.000)	1.879 \pm 0.014 (0.003)	2.216 \pm 0.003 (0.376)	0.527 \pm 0.028 (0.024)	0.428 \pm 0.020 (0.088)	0.992 \pm 0.019
	0.1	0.979 \pm 0.021 (0.087)	0.901 \pm 0.014 (0.001)	1.183 \pm 0.018 (0.032)	1.281 \pm 0.020 (0.137)	0.828 \pm 0.029 (0.053)	0.701 \pm 0.010 (0.085)	0.926 \pm 0.025
	0.15	0.953 \pm 0.024 (0.112)	0.850 \pm 0.022 (0.000)	1.014 \pm 0.011 (0.058)	1.017 \pm 0.026 (0.061)	0.940 \pm 0.027 (0.060)	0.839 \pm 0.004 (0.050)	0.681 \pm 0.020
UAS.4%, RA97.1%, TA84.4%	0.2	0.910 \pm 0.029 (0.120)	0.806 \pm 0.024 (0.007)	0.937 \pm 0.018 (0.091)	0.895 \pm 0.001 (0.041)	0.977 \pm 0.029 (0.043)	0.902 \pm 0.007 (0.033)	0.349 \pm 0.016
RL	0.05	0.974 \pm 0.011 (0.028)	0.953 \pm 0.005 (0.005)	26.032 \pm 0.008 (23.886)	23.369 \pm 0.008 (21.263)	0.038 \pm 0.015 (0.403)	0.038 \pm 0.016 (0.412)	0.994 \pm 0.010
	0.1	0.930 \pm 0.016 (0.038)	0.902 \pm 0.013 (0.003)	5.277 \pm 0.001 (4.055)	4.621 \pm 0.007 (3.410)	0.178 \pm 0.011 (0.552)	0.197 \pm 0.001 (0.545)	0.987 \pm 0.008
	0.15	0.875 \pm 0.011 (0.037)	0.856 \pm 0.008 (0.000)	1.758 \pm 0.004 (0.781)	1.657 \pm 0.005 (0.680)	0.496 \pm 0.006 (0.362)	0.516 \pm 0.009 (0.352)	0.970 \pm 0.017
UAI22.5%, RA93.5%, TA77.1%	0.2	0.810 \pm 0.006 (0.024)	0.805 \pm 0.013 (0.009)	1.147 \pm 0.005 (0.291)	1.144 \pm 0.003 (0.281)	0.707 \pm 0.004 (0.211)	0.707 \pm 0.013 (0.215)	0.945 \pm 0.005
GA	0.05	0.998 \pm 0.007 (0.052)	0.949 \pm 0.001 (0.001)	1.807 \pm 0.001 (0.339)	2.338 \pm 0.001 (0.232)	0.552 \pm 0.006 (0.111)	0.407 \pm 0.006 (0.043)	0.992 \pm 0.006
	0.1	0.986 \pm 0.009 (0.094)	0.890 \pm 0.007 (0.003)	1.147 \pm 0.003 (0.075)	1.278 \pm 0.007 (0.067)	0.863 \pm 0.008 (0.133)	0.703 \pm 0.002 (0.039)	0.918 \pm 0.010
	0.15	0.968 \pm 0.008 (0.130)	0.850 \pm 0.002 (0.003)	1.019 \pm 0.006 (0.038)	1.020 \pm 0.002 (0.043)	0.954 \pm 0.009 (0.096)	0.855 \pm 0.002 (0.033)	0.690 \pm 0.009
UAI3.9%, RA96.1%, TA84.2%	0.2	0.931 \pm 0.011 (0.145)	0.804 \pm 0.004 (0.008)	0.948 \pm 0.000 (0.092)	0.893 \pm 0.003 (0.030)	0.983 \pm 0.006 (0.065)	0.900 \pm 0.004 (0.022)	0.363 \pm 0.002
Teacher	0.05	0.967 \pm 0.013 (0.021)	0.950 \pm 0.017 (0.002)	6.465 \pm 0.007 (4.319)	6.233 \pm 0.004 (4.127)	0.151 \pm 0.002 (0.290)	0.151 \pm 0.006 (0.299)	0.990 \pm 0.014
	0.1	0.922 \pm 0.008 (0.030)	0.899 \pm 0.002 (0.000)	2.202 \pm 0.012 (0.980)	2.167 \pm 0.002 (0.956)	0.418 \pm 0.009 (0.312)	0.419 \pm 0.024 (0.323)	0.977 \pm 0.001
	0.15	0.869 \pm 0.025 (0.031)	0.852 \pm 0.002 (0.005)	1.467 \pm 0.015 (0.490)	1.459 \pm 0.004 (0.482)	0.591 \pm 0.005 (0.267)	0.581 \pm 0.001 (0.287)	0.958 \pm 0.021
SSD	0.05	0.999 \pm 0.001 (0.053)	0.952 \pm 0.000 (0.004)	1.346 \pm 0.001 (0.800)	1.824 \pm 0.000 (0.282)	0.742 \pm 0.000 (0.301)	0.522 \pm 0.001 (0.072)	0.986 \pm 0.001
	0.1	0.995 \pm 0.001 (0.052)	0.897 \pm 0.001 (0.002)	1.033 \pm 0.001 (0.189)	1.135 \pm 0.001 (0.076)	0.959 \pm 0.000 (0.229)	0.790 \pm 0.000 (0.048)	0.847 \pm 0.001
	0.15	0.918 \pm 0.020 (0.028)	0.801 \pm 0.017 (0.005)	1.129 \pm 0.005 (0.269)	1.138 \pm 0.001 (0.275)	0.718 \pm 0.017 (0.200)	0.704 \pm 0.009 (0.218)	0.927 \pm 0.017
NegGrad+	0.05	0.999 \pm 0.000 (0.053)	0.979 \pm 0.001 (0.031)	0.946 \pm 0.002 (1.200)	1.443 \pm 0.004 (0.663)	1.056 \pm 0.002 (0.615)	0.678 \pm 0.012 (0.228)	0.992 \pm 0.001
	0.1	0.996 \pm 0.000 (0.104)	0.946 \pm 0.002 (0.047)	0.900 \pm 0.003 (0.322)	1.078 \pm 0.006 (0.134)	1.107 \pm 0.005 (0.377)	0.877 \pm 0.003 (0.135)	0.933 \pm 0.003
	0.15	0.990 \pm 0.000 (0.152)	0.900 \pm 0.003 (0.052)	0.853 \pm 0.004 (0.124)	1.008 \pm 0.002 (0.031)	1.161 \pm 0.005 (0.303)	0.892 \pm 0.001 (0.025)	0.712 \pm 0.015
UAI11.5%, RA98.7%, TA83.8%	0.2	0.814 \pm 0.020 (0.128)	0.801 \pm 0.017 (0.005)	1.129 \pm 0.005 (0.269)	1.138 \pm 0.001 (0.275)	0.718 \pm 0.017 (0.200)	0.704 \pm 0.009 (0.218)	0.927 \pm 0.017
Salun	0.05	0.999 \pm 0.001 (0.053)	0.979 \pm 0.001 (0.031)	0.946 \pm 0.002 (1.200)	1.443 \pm 0.028 (0.663)	1.056 \pm 0.002 (0.615)	0.678 \pm 0.012 (0.228)	0.992 \pm 0.001
	0.1	0.976 \pm 0.011 (0.084)	0.924 \pm 0.039 (0.026)	1.386 \pm 0.422 (0.164)	1.579 \pm 0.136 (0.368)	0.764 \pm 0.295 (0.034)	0.590 \pm 0.077 (0.152)	0.973 \pm 0.002
	0.15	0.944 \pm 0.024 (0.106)	0.876 \pm 0.046 (0.029)	1.054 \pm 0.175 (0.162)	1.139 \pm 0.175 (0.162)	0.920 \pm 0.195 (0.062)	0.770 \pm 0.051 (0.098)	0.942 \pm 0.002
UAI9.2%, RA95.7%, TA81.9%	0.2	0.900 \pm 0.044 (0.114)	0.825 \pm 0.049 (0.029)	0.910 \pm 0.097 (0.054)	0.969 \pm 0.037 (0.105)	1.000 \pm 0.164 (0.082)	0.851 \pm 0.020 (0.071)	0.893 \pm 0.002
SFRon	0.05	0.994 \pm 0.001 (0.048)	0.947 \pm 0.003 (0.001)	2.010 \pm 0.188 (0.136)	2.422 \pm 0.087 (0.222)	0.497 \pm 0.042 (0.057)	0.407 \pm 0.016 (0.043)	0.983 \pm 0.002
	0.1	0.980 \pm 0.006 (0.087)	0.900 \pm 0.003 (0.001)	1.245 \pm 0.060 (0.023)	1.338 \pm 0.039 (0.126)	0.788 \pm 0.041 (0.058)	0.673 \pm 0.020 (0.069)	0.909 \pm 0.003
	0.15	0.951 \pm 0.011 (0.113)	0.849 \pm 0.003 (0.001)	1.041 \pm 0.020 (0.065)	1.044 \pm 0.023 (0.067)	0.913 \pm 0.028 (0.055)	0.813 \pm 0.016 (0.055)	0.738 \pm 0.029
UAI6.3%, RA96.8%, TA82.9%	0.2	0.910 \pm 0.011 (0.125)	0.803 \pm 0.003 (0.008)	0.947 \pm 0.006 (0.091)	0.910 \pm 0.022 (0.046)	0.961 \pm 0.017 (0.044)	0.884 \pm 0.017 (0.038)	0.523 \pm 0.068

1161
1162
1163
1164
1165
1166
1167
1168
1169
1170
1171
1172
1173
1174
1175
1176
1177
1178
1179
1180
1181
1182
1183
1184
1185
1186
1187

Table 16: Unlearning performance of 9 unlearning methods on Tiny ImageNet with ViT in class-wise forgetting scenario.

Methods	α	Coverage		Set Size		CR		\hat{q}_f	\hat{q}_{test}
		$\mathcal{D}_f \downarrow$	$\mathcal{D}_{test} \uparrow$	$\mathcal{D}_f \uparrow$	$\mathcal{D}_{test} \downarrow$	$\mathcal{D}_f \downarrow$	$\mathcal{D}_{test} \uparrow$		
RT	0.05	1.000 \pm 0.000 (0.000)	0.950 \pm 0.003 (0.000)	200.000 \pm 0.000 (0.000)	1.785 \pm 0.000 (0.000)	0.005 \pm 0.000 (0.000)	0.005 \pm 0.000 (0.000)	0.532 \pm 0.009 (0.000)	1.000 \pm 0.000 0.984 \pm 0.002
	0.1	0.936 \pm 0.011 (0.000)	0.960 \pm 0.004 (0.000)	192.882 \pm 0.012 (0.000)	1.84340 \pm 0.020 (0.000)	0.005 \pm 0.000 (0.000)	0.005 \pm 0.000 (0.000)	0.788 \pm 0.008 (0.000)	1.000 \pm 0.000 0.859 \pm 0.004
	0.15	0.900 \pm 0.009 (0.000)	0.953 \pm 0.003 (0.000)	188.534 \pm 0.010 (0.000)	1.84340 \pm 0.020 (0.000)	0.005 \pm 0.000 (0.000)	0.005 \pm 0.000 (0.000)	0.788 \pm 0.008 (0.000)	1.000 \pm 0.000 0.859 \pm 0.004
UAI100%, UA86.4%	0.2	0.757 \pm 0.001 (0.000)	0.860 \pm 0.024 (0.000)	171.051 \pm 0.011 (0.000)	171.480 \pm 0.211 (0.000)	0.005 \pm 0.000 (0.000)	0.005 \pm 0.000 (0.000)	0.936 \pm 0.002 (0.000)	1.000 \pm 0.000 0.232 \pm 0.001
FT	0.05	0.993 \pm 0.003 (0.047)	0.962 \pm 0.026 (0.014)	3.284 \pm 0.208 (1.138)	4.112 \pm 0.813 (2.007)	0.500 \pm 0.478 (0.059)	0.241 \pm 0.057 (0.209)	0.989 \pm 0.001	
	0.1	0.976 \pm 0.011 (0.084)	0.924 \pm 0.039 (0.026)	1.386 \pm 0.422 (0.164)	1.579 \pm 0.136 (0.368)	0.546 \pm 0.541 (0.141)	0.518 \pm 0.009 (0.153)	0.698 \pm 0.019 (0.060)	0.971 \pm 0.019 0.924 \pm 0.016
	0.15	0.944 \pm 0.024 (0.106)	0.876 \pm 0.046 (0.029)	1.054 \pm 0.175 (0.162)	1.139 \pm 0.175 (0.162)	0.607 \pm 0.607 (0.067)	0.585 \pm 0.022 (0.057)	0.809 \pm 0.010 (0.084)	0.912 \pm 0.015 0.868 \pm 0.004
RL	0.05	0.994 \pm 0.001 (0.048)	0.960 \pm 0.020 (0.000)	2.000 \pm 0.000 (0.000)	2.000 \pm 0.000 (0.000)	0.005 \pm 0.000 (0.000)	0.005 \pm 0.000 (0.000)	0.532 \pm 0.009 (0.000)	1.000 \pm 0.000 0.984 \pm 0.002
	0.1	0.984 \pm 0.001 (0.048)	0.930 \pm 0.017 (0.000)	180.412<					

Table 17: MIACR performance on CIFAR-10 with ResNet-18.

Methods	α	10% Forgetting		50% Forgetting	
		MIACR \uparrow	\hat{q}	MIACR \uparrow	\hat{q}
RT	0.05	0.089 \pm 0.001(0.000)	0.877 \pm 0.004	0.117 \pm 0.010(0.000)	0.899 \pm 0.007
	0.1	0.147 \pm 0.000(0.000)	0.589 \pm 0.008	0.201 \pm 0.011(0.000)	0.570 \pm 0.001
	0.15	0.203 \pm 0.010(0.000)	0.485 \pm 0.005	0.272 \pm 0.011(0.000)	0.472 \pm 0.009
MIA86.92% (10% Forgetting)	0.2	0.246 \pm 0.000(0.000)	0.473 \pm 0.001	0.318 \pm 0.006(0.000)	0.459 \pm 0.003
	0.05	0.037 \pm 0.011(0.052)	0.745 \pm 0.013	0.038 \pm 0.001(0.079)	0.780 \pm 0.011
	0.1	0.077 \pm 0.008(0.070)	0.627 \pm 0.000	0.103 \pm 0.011(0.098)	0.558 \pm 0.012
FT	0.15	0.128 \pm 0.007(0.075)	0.517 \pm 0.006	0.159 \pm 0.011(0.113)	0.494 \pm 0.011
	0.2	0.196 \pm 0.003(0.050)	0.483 \pm 0.000	0.244 \pm 0.010(0.074)	0.476 \pm 0.004
	0.05	0.056 \pm 0.010(0.033)	0.627 \pm 0.011	0.057 \pm 0.016(0.060)	0.547 \pm 0.000
RL	0.1	0.178 \pm 0.027(0.031)	0.572 \pm 0.005	0.137 \pm 0.030(0.064)	0.547 \pm 0.001
	0.15	0.272 \pm 0.006(0.069)	0.492 \pm 0.015	0.194 \pm 0.031(0.078)	0.547 \pm 0.001
	0.2	0.320 \pm 0.025(0.074)	0.485 \pm 0.011	0.261 \pm 0.001(0.057)	0.546 \pm 0.000
GA	0.05	0.010 \pm 0.002(0.079)	0.862 \pm 0.016	0.010 \pm 0.019(0.107)	0.771 \pm 0.008
	0.1	0.032 \pm 0.003(0.115)	0.502 \pm 0.016	0.055 \pm 0.003(0.146)	0.486 \pm 0.005
	0.15	0.076 \pm 0.000(0.127)	0.477 \pm 0.007	0.107 \pm 0.016(0.165)	0.474 \pm 0.015
MIA98.80% (10% Forgetting)	0.2	0.146 \pm 0.016(0.100)	0.476 \pm 0.019	0.164 \pm 0.016(0.154)	0.473 \pm 0.011
	0.05	0.011 \pm 0.006(0.078)	0.750 \pm 0.014	0.031 \pm 0.003(0.086)	0.635 \pm 0.018
	0.1	0.038 \pm 0.023(0.109)	0.672 \pm 0.028	0.065 \pm 0.021(0.136)	0.582 \pm 0.013
MIA93.24% (50% Forgetting)	0.15	0.072 \pm 0.013(0.131)	0.625 \pm 0.029	0.110 \pm 0.017(0.162)	0.548 \pm 0.007
	0.2	0.113 \pm 0.008(0.133)	0.588 \pm 0.019	0.159 \pm 0.017(0.159)	0.532 \pm 0.006
	0.05	0.010 \pm 0.011(0.079)	0.861 \pm 0.012	0.011 \pm 0.002(0.106)	0.748 \pm 0.011
SSD	0.1	0.031 \pm 0.010(0.116)	0.511 \pm 0.011	0.051 \pm 0.005(0.150)	0.488 \pm 0.001
	0.15	0.077 \pm 0.005(0.126)	0.480 \pm 0.013	0.104 \pm 0.006(0.168)	0.477 \pm 0.015
	0.2	0.139 \pm 0.011(0.107)	0.475 \pm 0.013	0.168 \pm 0.012(0.150)	0.477 \pm 0.006
NegGrad+	0.05	0.076 \pm 0.025(0.013)	0.844 \pm 0.024	0.045 \pm 0.008(0.072)	0.863 \pm 0.025
	0.1	0.128 \pm 0.018(0.019)	0.481 \pm 0.000	0.109 \pm 0.007(0.092)	0.511 \pm 0.008
	0.15	0.174 \pm 0.022(0.029)	0.480 \pm 0.005	0.167 \pm 0.017(0.105)	0.477 \pm 0.010
MIA93.82% (50% Forgetting)	0.2	0.213 \pm 0.012(0.033)	0.480 \pm 0.004	0.230 \pm 0.014(0.088)	0.472 \pm 0.008
Salun	0.05	0.055 \pm 0.014(0.034)	0.691 \pm 0.011	0.044 \pm 0.001(0.073)	0.670 \pm 0.008
	0.1	0.113 \pm 0.009(0.034)	0.681 \pm 0.013	0.115 \pm 0.009(0.086)	0.630 \pm 0.009
	0.15	0.198 \pm 0.006(0.005)	0.642 \pm 0.015	0.170 \pm 0.009(0.102)	0.610 \pm 0.003
MIA59.12% (50% Forgetting)	0.2	0.267 \pm 0.009(0.021)	0.608 \pm 0.011	0.220 \pm 0.005(0.098)	0.586 \pm 0.005
SFRon	0.05	0.060 \pm 0.001(0.029)	0.711 \pm 0.009	0.058 \pm 0.002(0.059)	0.715 \pm 0.008
	0.1	0.040 \pm 0.004(0.107)	0.626 \pm 0.025	0.046 \pm 0.002(0.155)	0.562 \pm 0.013
	0.15	0.113 \pm 0.003(0.090)	0.517 \pm 0.003	0.134 \pm 0.013(0.138)	0.498 \pm 0.003
MIA91.55% (10% Forgetting)	0.2	0.184 \pm 0.002(0.062)	0.487 \pm 0.002	0.206 \pm 0.014(0.112)	0.483 \pm 0.002
MIA92.52% (50% Forgetting)	0.05	0.060 \pm 0.001(0.029)	0.711 \pm 0.009	0.058 \pm 0.002(0.059)	0.715 \pm 0.008
	0.1	0.040 \pm 0.004(0.107)	0.626 \pm 0.025	0.046 \pm 0.002(0.155)	0.562 \pm 0.013
	0.15	0.113 \pm 0.003(0.090)	0.517 \pm 0.003	0.134 \pm 0.013(0.138)	0.498 \pm 0.003
MIA92.52% (50% Forgetting)	0.2	0.184 \pm 0.002(0.062)	0.487 \pm 0.002	0.206 \pm 0.014(0.112)	0.483 \pm 0.002

Table 18: Performance of our unlearning framework. We show the unlearning performance on CIFAR-10 with ResNet-18 and Tiny ImageNet with ViT in 10% random data forgetting scenario.

Methods	α	UA \uparrow	RA \uparrow	$\lambda = 0.2$	TA \uparrow	CR _{D_T} \downarrow	CR _{D_{test}} \uparrow	UA \uparrow	RA \uparrow	$\lambda = 0.5$	TA \uparrow	CR _{D_T} \downarrow	CR _{D_{test}} \uparrow	UA \uparrow	RA \uparrow	$\lambda = 1$	TA \uparrow	CR _{D_T} \downarrow	CR _{D_{test}} \uparrow	
		CIFAR-10 with ResNet-18																		
RT	0.05	0.788 \pm 0.076(0.055)	0.824 \pm 0.055			0.763 \pm 0.101(0.054)	0.825 \pm 0.054			0.719 \pm 0.145(0.059)	0.820 \pm 0.059									
	0.1	10.8%(2.2)	98.3%(1.4)	91.0%(0.8)	0.914(0.029)	0.924(0.021)		14.0%(5.4)	97.8%(1.9)	90.4%(0.4)	0.879 \pm 0.064(0.033)	0.912 \pm 0.033		17.7%(9.1)	96.8%(2.9)	90.5%(1.3)	0.838 \pm 0.105(0.034)	0.911 \pm 0.034		
	0.15				0.956 \pm 0.019(0.009)	0.959 \pm 0.009		0.977 \pm 0.011(0.005)	0.976 \pm 0.005		0.936 \pm 0.039(0.014)	0.954 \pm 0.014				0.906 \pm 0.069(0.017)	0.951 \pm 0.017	0.932 \pm 0.056(0.016)	0.965 \pm 0.016	
FT	0.05	0.844 \pm 0.020(0.050)	0.829 \pm 0.050			0.853 \pm 0.011(0.036)	0.843 \pm 0.036			0.835 \pm 0.029(0.025)	0.854 \pm 0.025									
	0.1	6.8%(1.8)	97.0%(2.7)	90.8%(1.0)	0.948 \pm 0.005(0.021)	0.924 \pm 0.021		7.9%(0.7)	96.9%(2.8)	90.9%(0.9)	0.940 \pm 0.003(0.027)	0.927 \pm 0.018		9.2%(0.6)	97.9%(1.8)	91.2%(0.6)	0.938 \pm 0.005(0.025)	0.936 \pm 0.009		
	0.2				0.989 \pm 0.001(0.007)	0.974 \pm 0.007					0.983 \pm 0.005(0.006)	0.975 \pm 0.006				0.986 \pm 0.002(0.002)	0.984 \pm 0.003			
RL	0.05	0.709 \pm 0.155(0.736)(0.143)	0.736 \pm 0.143			0.708 \pm 0.156(0.731)(0.148)	0.731 \pm 0.148			0.629 \pm 0.235(0.669)(0.210)	0.669 \pm 0.210									
	0.1	9.7%(1.1)	96.6%(3.1)	89.4%(2.4)	0.896 \pm 0.047(0.887)(0.058)	0.887 \pm 0.058		9.9%(1.3)	96.9%(2.8)	89.7%(2.1)	0.902 \pm 0.041(0.896)(0.049)	0.896 \pm 0.049		12.6%(4.0)	95.3%(4.4)	88.1%(3.7)	0.845 \pm 0.098(0.858)(0.087)	0.911 \pm 0.064(0.913)(0.055)		0.936 \pm 0.052(0.938)(0.043)
	0.15				0.946 \pm 0.029(0.931)(0.037)	0.931 \pm 0.037		0.964 \pm 0.024(0.949)(0.032)	0.949 \pm 0.032		0.959 \pm 0.029(0.950)(0.031)	0.950 \pm 0.031								
Tiny ImageNet with ViT	RT	0.05	0.458 \pm 0.045(0.516)(0.000)	0.516 \pm 0.000			0.306 \pm 0.107(0.489)(0.027)	0.489 \pm 0.027			0.346 \pm 0.157(0.481)(0.035)	0.481 \pm 0.035								
	0.1	19.3%(4.6)	98.8%(0.0)	86.0%(0.0)	0.841 \pm 0.046(0.786)(0.000)	0.786 \pm 0.000		0.841 \pm 0.046(0.889)(0.000)	0.889 \pm 0.000		0.649 \pm 0.126(0.765)(0.021)	0.765 \pm 0.021		35.7%(21.0)	98.6%(0.2)	85.2%(0.8)	0.549 \pm 0.226(0.739)(0.047)	0.658 \pm 0.222(0.861)(0.028)		
	0.2				0.898 \pm 0.036(0.932)(0.003)	0.932 \pm 0.003					0.839 \pm 0.095(0.929)(0.006)	0.929 \pm 0.006				0.743 \pm 0.191(0.918)(0.017)				
FT	0.05	0.441 \pm 0.062(0.399)(0.117)	0.399 \pm 0.117			0.413 \pm 0.090(0.401)(0.115)	0.401 \pm 0.115			0.342 \pm 0.161(0.363)(0.153)	0.363 \pm 0.153									
	0.1	9.8%(4.9)	97.4%(1.4)	83.6%(2.4)	0.884 \pm 0.004(0.823)(0.066)	0.823 \pm 0.066		13.6%(0.9)	97.2%(1.6)	83.6%(2.4)	0.718 \pm 0.057(0.683)(0.033)	0.683 \pm 0.033		20.0%(5.3)	96.4%(2.4)	82.9%(3.1)	0.627 \pm 0.148(0.652)(0.134)	0.772 \pm 0.108(0.802)(0.087)		
	0.2				0.942 \pm 0.008(0.893)(0.042)	0.893 \pm 0.042					0.914 \pm 0.020(0.890)(0.045)	0.890 \pm 0.045				0.856 \pm 0.078(0.877)(0.058)				
RL	0.05	0.051 \pm 0.452(0.111)(0.405)	0.111 \pm 0.405			0.051 \pm 0.452(0.121)(0.395)	0.121 \pm 0.395			0.048 \pm 0.455(0.119)(0.397)	0.119 \pm 0.397									
	0.15	31.8%(17.1)	95.3%(17.9)	80.9%(5.1)	0.278 \pm 0.497(0.451)(0.335)	0.451 \pm 0.335		36.2%(21.5)	95.3%(3.5)	80.4%(5.6)	0.254 \pm 0.521(0.449)(0.337)	0.449 \pm 0.337		40.2%(25.5)	94.5%(4.3)	79.5%(6.5)				